

# ELEC6089 High Voltage Insulation Systems Assignment 1

## HV AC 275kV Bushing Design

Thomas J. Smith, David Mahmoodi, Brendan Hickman, Patrick P. L. Fong

University of Southampton

March 25, 2014

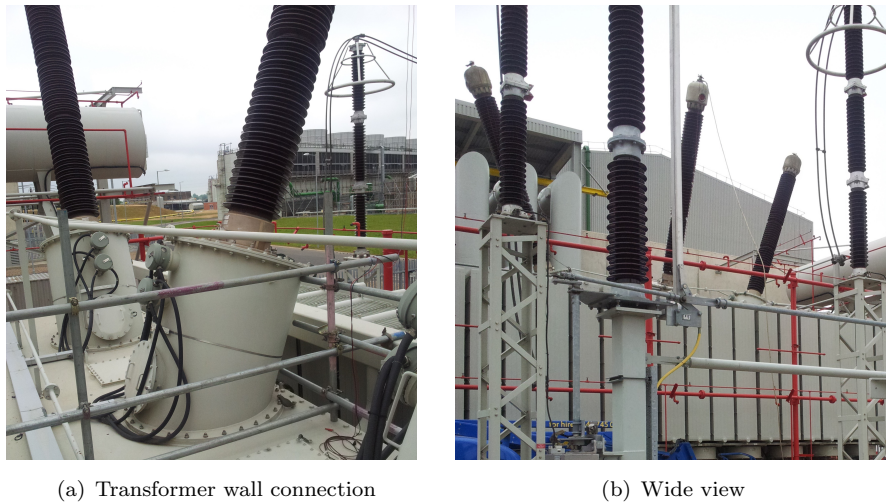
### Abstract

*The advantages to work in high voltages come with drawbacks, one of the major drawbacks is the increase in complexity of required insulation system associated with voltage level. In high voltage transformer, bushings are required to avoid various electrical breakdown mechanisms caused by the potential difference from equipments to the surrounding earth objects i.e. transformer casing. This report start by discussing the different types of breakdown in high voltage systems and the stress control methods used in relatively lower voltages and DC systems. High voltage AC solutions are discussed, derivation of capacitive stress control in bushing designs and simulated to illustrate the effects of the the two capacitive stress control methods.*

## 1 Introduction

The design of electrical equipment always involves an aspect of insulation design. For the safe and efficient operation of electrical equipment it is necessary to have an electrical circuit and a means of isolating this circuit from the surrounding environment [1]. Power systems contain a complex structure of generators, transmission lines, transformers, switchgear and other equipment. All of these different devices require an appropriately selected insulation material in order to isolate the mechanical casings and support structures from the high voltage components [2].

The purpose of this report is to describe the design and simulation of a high voltage bushing. Bushings are an integral part of power system insulation. IEEE standard C57.19.00 describes a bushing as “an insulating structure, including a through conductor or providing a central passage for such a conductor, with provision for mounting on a barrier, conducting or otherwise, for the purpose of insulating the conductor from the barrier and conducting current from one side of the barrier to the other.”[3]. Bushings are required for situations such as connecting the external conductor to the internal windings of a transformer through the walls of the metal oil tank. The walls of the transformer housing will be grounded, but need to be shielded from the incoming high voltage conductor, hence the use of an insulating bushing [1]. An example of this application can be seen in figure 1.1, as 400kV grid conductors enter an oil filled transformer casing. The shedding on the outer cylinder can be seen in figure 1.1 which helps increase electrical strength in wet conditions [1].



(a) Transformer wall connection

(b) Wide view

Figure 1.1: High Voltage Bushings on the 400kV Transformers at Staythorpe CCGT Power Station, Newark, UK (Photos: Thomas J. Smith)

## 2 Overview of Insulation Failure

There are some consequences that need to be taken into account when designing systems for operation at high voltage. High voltage systems generate a higher electric potential than surrounding objects, which are usually at earth potential. These arise large electric potential gradients or electric fields. The values of high field regions within the electric field may cause electrical breakdown and partial discharges leading to failure of the system [4]. It is therefore important to design systems to minimise the chance of these events.

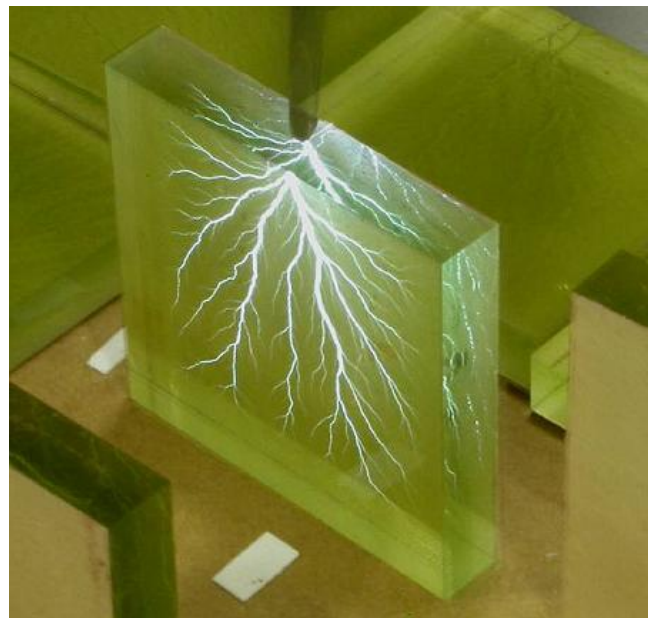


Figure 2.1: Electrical tree tracing the path of damaged insulation caused by electrical breakdown [5]

Electrical breakdown is the action of electrical conduction across an insulating medium, usually a dielectric, following the voltage across this medium exceeding the breakdown voltage of the specific material. This usually happens when the potential difference is extremely high and arcing can be seen

in gaseous insulating mediums. This can cause changes to the compounds in the insulating medium and also cause damage to equipment in the form of treeing as shown in figure 2.1.

There are different types of electrical breakdown to consider. The main types of electrical breakdown that are involved in high voltage insulation systems are general breakdown in the system, surface flashover, partial discharge in the dielectric insulation as well as corona discharge in air.

## 2.1 General Breakdown

In the case of a high voltage transformer bushing, there is a combination of both high electric fields and a close proximity to the grounded surroundings. As mentioned in section 1, the purpose of a bushing is to insulate the conductor from ground. The most basic form of bushing is a non-condenser bushing [6]. It is the radial component of the tangential electric field that causes this typical breakdown directly from the conductor to the grounded flange. Insulation must have a very high dielectric constant to withstand high voltage conditions. Typical materials used for bushing manufacture include Resin-impregnated paper (RIP) and Oil-impregnated paper (OIP). The importance of this type of bushing is that as the electric strength of the insulation increases, radial thickness may be reduced [6]. Typically the general breakdown strength of bushings is very high relative to PD inception and is only a secondary concern.

## 2.2 Surface Flashover

The partnering electric breakdown effect for solid, non-condenser bushing is surface flashover; breakdown caused by the electric field travelling from the conductor to the surroundings via the surface of the bushing. The properties governing the axial height of the bushing are both the axial electric field and the surrounding medium [6]. Typically the criteria for surface flashover breakdown is much lower than general breakdown, and improvements to the bushing have primarily been in shaping the axial field distribution. This investigation considers an air-to-oil bushing and as oil is more than twice as strong dielectrically as air at atmospheric pressure the air end must be approximately twice as long [7]. Creepage distance is a critical factor here, as defined in the IEC 60137 standard as the “shortest distance along the surface of an insulator between two conductive parts” [8]. For industrial standard bushings, ceramic shedding is used to extend the length of the surface of the bushing. While this is beyond the scope of this report and therefore not modelled, it is important to note that it will typically increase the effective axial length of the bushing by a factor of 4.

## 2.3 Partial Discharge

Partial Discharge (PD) is defined by the British Standards 60270:2001 as a localized electrical discharge that only partially bridges the insulation between conductors and which can, or can not, occur adjacent to a conductor and as a consequence of local electrical stress concentrations in the insulation [9]. The most common cause of partial discharge is a void, originating from manufacturing imperfections, within the dielectric material where the void contains material of a lower electrical breakdown strength (gas or air) than the dielectric material. Under high electric fields across the dielectric insulation these voids will experience local electrical breakdown as the rate of charge increase is greater than decay and inception voltage is exceeded. Due to these conditions, PDs typically occur under intense tangential electric field resulting in electron emission [10] and as the discharges spread across the surface of the solid dielectric breakdown will occur [4]. In order to ensure the insulation system can sufficiently

reduce the chance of PD, the inception voltage of the insulation must be relatively high compare to the operating voltage of the conductor.

Partial discharge is a primary cause of ageing within High Voltage systems, this is because each successive discharge applies electro-mechanical forces to the void itself and the insulation progressively deteriorates [11]. Therefore reducing tangential electric fields and measurement of PDs is of high importance.

## 2.4 Corona Discharge

Corona discharge is the ionisation of fluid around a conductor of high electric potential creating a high electric field ionisation region [12]. The ionisation of the surrounding fluid is due to the discharge from the conductor. In high voltage systems, corona discharge occurs most commonly from the conductor to air surrounding the conductor as illustrated in figure 2.2. Corona discharge occurs at an area of intense electric field, but not sufficiently intense to cause arcing. This type of breakdown might not cause fatal damage to the insulation, but would shorten the life time of the insulation system. It also represents power losses to the surrounding, so it is important to design insulation system minimising the effect of corona discharge.

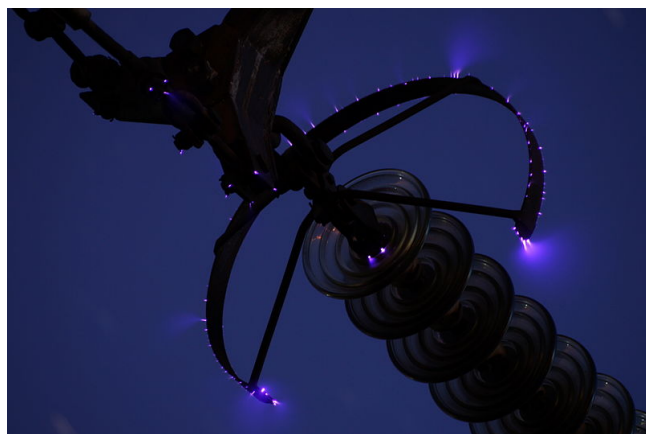


Figure 2.2: Corona discharge appearing on the insulation surface of high voltage conductor

## 3 Grading Methods

Electric field stress control is important in the design of many power system elements, especially cable terminations and bushings [2]. Failure of a bushing can damage the power transformer it is protecting, which can be an expensive mistake [1]. Bushings are required to withstand Electrical, Mechanical and Thermal stresses as defined in the IEEE standard C57.19.00 [3]. The design of the bushing is largely determined by the insulation material chosen and the resolution of these conflicting sources of stress. A good bushing design has insulation that can withstand the applied voltage and thermal characteristics appropriate for the current carried by the conductor [7].

The problem grading methods attempt to resolve is laid out in figure 3.1. The grounded transformer casing is shown in light grey which is perpendicular to the the bushing insulation shown in dark grey and the high voltage conductor in white. The top of the bushing is exposed to air, while the other side is exposed to transformer oil. Conducting a numerical analysis or simulation would show that the conductor surface within the plane of the transformer casing and at the points marked by red

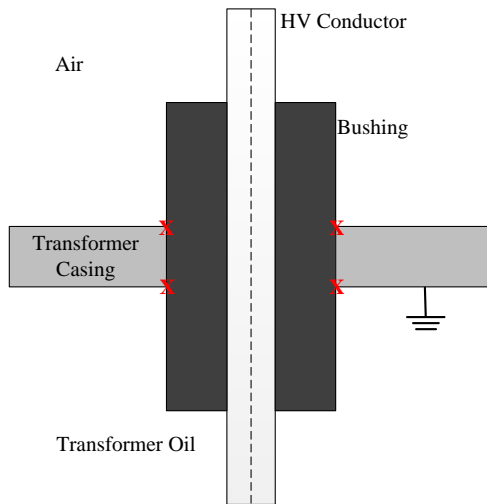


Figure 3.1: The Bushing Problem

crosses would experience high electric field stress. The bushing insulation is designed to withstand the high electric field between the conductor and the transformer casing, however at the points marked with crosses the interface between the solid insulation and the air/transformer oil would cause surface discharge leading to relatively low flashover voltages [4]. It is therefore necessary to develop methods of reducing electric field stress to a more uniform distribution for both functional purposes and the economic use of space and materials [2].

### 3.1 Overview of Low Voltage and DC Solutions

There are several methods that can be used dependent upon the application. Low voltage solutions include internal and external screening electrodes, while resistive stress control can be used for DC applications. Sometimes these solutions are used in combination to achieve an acceptable result.

#### 3.1.1 External Screening Electrode

External screening electrodes are parts outside the conductor that are not electrically connected to the conductor. They are made of metal conductors such as aluminium. Corona ring designs are intended to reduce the electric field strength around the bushing terminal, hence reducing the chance of corona or partial discharge. Grading ring designs are intended to reduce the potential gradient of insulator, hence reducing the chance of electrical breakdown. These screening electrodes come with various shapes according to the different designs. The main types of design take the shape of sphere, toroid or ring. These are shapes which prevent regions of intense electric field strength by varying the electric potential distribution and help contain electric field as much as possible. The reduction in corona discharge not only reduces the power loss, it also suppresses the ageing speed of the insulator. An example of these can be seen on figure 1.1(a) and figure 1.1(b), where they are placed at the top of the bushings. The diameters of these designs are closely related to the electric field strength around the electrode, so the diameters of these designs must be carefully considered in order to avoid electrical breakdown.

### 3.1.2 Internal Screening Electrode

Internal screening electrodes are also used to control the electric potential distribution so the electric field strength is within acceptable level to reduce the chance of breakdown. They are placed inside the insulator and usually in a pressurised gas. Some existing designs have the shape of the internal electrode as a 3D cone and is referred to as a deflector. There are also designs which are disk shape. An example of the field distribution with the cone shape deflector inserted is demonstrated in figure 3.2.

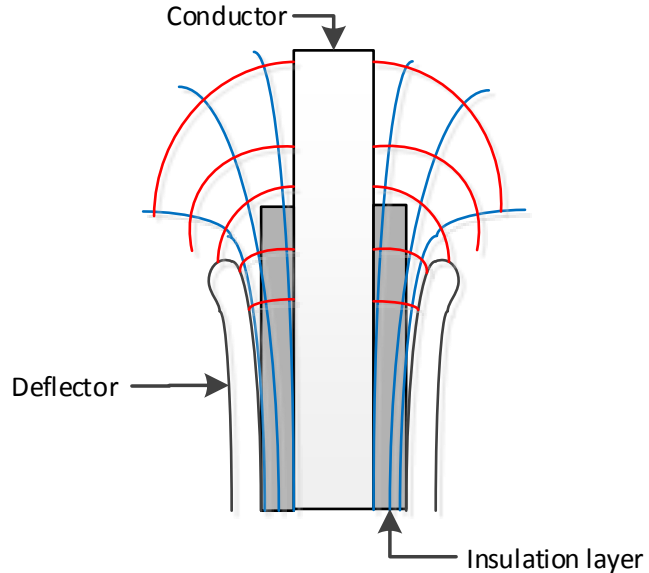


Figure 3.2: Field distribution with deflector

## 3.2 Capacitive Grading

Capacitive grading was first proposed by R.Nagel of Siemens in a German paper published in 1906 [7]. The value of this type of arrangement was quickly recognised, and is now industry standard practice for AC bushing designs for 25kV - 1500kV applications [2]. The general concept of the design is illustrated in figure 3.3, showing the isolated foils inserted inside the solid bushing insulation. Shown in red in figure 3.3 is the potential field with no grading, and in blue with the isolated conductive foils inserted. It shows that the whole dielectric is much more evenly stressed with the capacitive grading method.

The insulation is stressed in both radial and axial directions, which sum to give the tangential field. The radial component  $E_r$  can cause breakdown of the insulating material, while the axial component  $E_z$  can cause surface discharge along the boundary [13]. Attention must be paid to the design and shape of the boundary, so that the critical value for inception voltage for surface discharge is not exceeded [14]. These can be seen in green in figure 3.3. These sum to give the tangential field  $E_t$  at any point in the design.

Before proceeding, it is first necessary to introduce some terms. Firstly, the radius of the foil is referenced from the centre of the conductor, and termed  $r_n$ . The spacing between each foil is defined in equation 1.

$$S_n = r_n - r_{n-1} \quad (1)$$

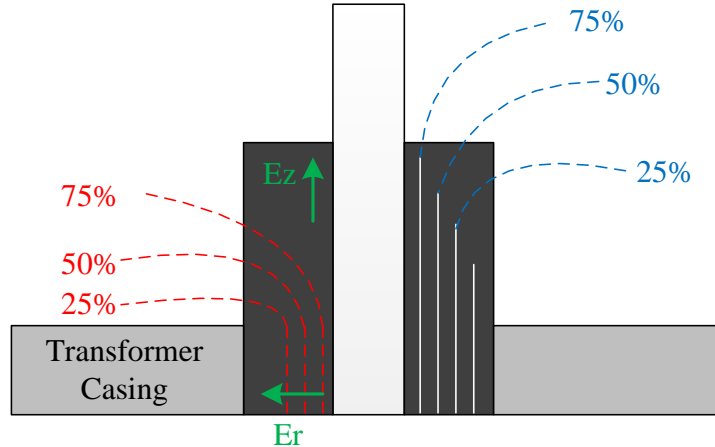


Figure 3.3: Field Distribution both without capacitive grading (shown in red) and with capacitive grading (shown in blue), modified from [2]

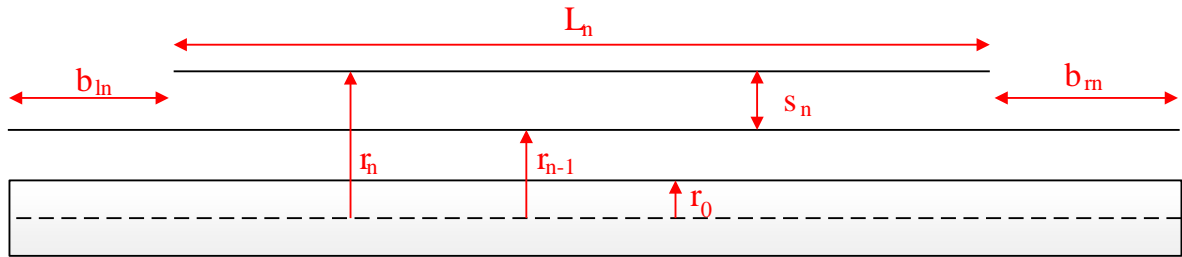


Figure 3.4: Symbols for calculating capacitive grading, modified from [13]

Additionally, the length of each foil is referred to as  $L_n$  and the difference in length on the right and left side between each foil is termed  $b_{ln}$  and  $b_{rn}$ . Symmetric double sided capacitive grading is achieved when  $b_{ln} = b_{rn}$  [13]. The total number of foils in the system is  $N$ . Also note that subscript  $n$  denotes the outermost foil.

Inserting isolated conducting foils forms a set of coaxial capacitor units [4]. The equation for the capacitance of one of these capacitors depends on the radial displacement  $r_n$  and length of each foil  $L_n$ , as in equation 2.

$$C_n = \frac{2\pi\epsilon L_n}{\ln\left(\frac{r_n}{r_{n-1}}\right)} \quad (2)$$

The most widely used method to choose the dimensions and locations of the foils is double sided capacitive grading, of which there are two variants; radial grading and axial grading [13]. The aim of capacitive grading is to evenly distribute the electric field between the foils. To achieve this, an even voltage difference between foils is required as in equation 3, where  $V$  is the total voltage difference between the conductor and the casing,  $N$  is the number of foils required and  $\Delta V$  is the voltage

difference between each consecutive pair of foils [15].

$$\Delta V = \frac{V}{N} \quad (3)$$

For the voltage between each foil to be constant, as in equation 3, the capacitance between each consecutive pair of foils must also be constant. This is expressed as  $C_n = C_{n-1} = \dots = C_0$

### 3.2.1 Radial Grading

The radial spacing and dimension of each foil is determined in the following derivation, which has been verified and modified from [4]. In radial grading, the radial component of the electric field  $E_r$  is kept constant between all consecutive foils. The radial electric field is related to the voltage difference and the spacing between each foil, as in equation 4.  $\Delta V$  is already defined as a constant from equation 3, and so to have equal field the foil spacing  $S_n$  should also be constant.

$$E_r = \frac{\Delta V}{S_n} = \text{Constant} \quad (4)$$

Given this condition and equation 2 for coaxial capacitance, the length of each foil is required to change from foil to foil. The lengths and radii of consecutive foils can be calculated from the relationship in equation 5.

$$C_n = \frac{2\pi\epsilon L_n}{\ln(\frac{r_n}{r_{n-1}})} = C_{n-1} = \frac{2\pi\epsilon L_{n-1}}{\ln(\frac{r_{n-1}}{r_{n-2}})} = \dots = C_1 = \frac{2\pi\epsilon L_1}{\ln(\frac{r_1}{r_0})} \quad (5)$$

The common factor of  $2\pi\epsilon$  cancels from equation 5 giving a simple equation linking the lengths and radial displacements of consecutive foils, as in equation 6.

$$\frac{L_n}{\ln(\frac{r_n}{r_{n-1}})} = \frac{L_{n-1}}{\ln(\frac{r_{n-1}}{r_{n-2}})} = \dots = \frac{L_1}{\ln(\frac{r_1}{r_0})} \quad (6)$$

An approximate solution for thin foils can then be found. Under the thin foil assumption,  $r_n = r_{n-1} + S_n$  and  $\frac{S_n}{r_n} \ll 1$  even for the smallest radii of the inner foil. This is shown in equation 8.

$$\ln(\frac{r_n}{r_{n-1}}) = \ln \frac{1}{1 - (\frac{S_n}{r_n})} \approx \frac{S_n}{r_n} \quad (7)$$

$$L_n r_n \approx L_{n-1} r_{n-1} \approx \dots \approx L_1 r_1 \quad (8)$$

Equation 6 can then be used to determine an exact solution while equation 8 can be used to find an approximate solution in conjunction with initial data regarding the length and radial displacement of the first foil and the spacing of the foils to calculate the parameters of all the other foils in the bushing. Nevertheless, it should be noted, at this stage, that  $r_0$  refers to the surface of the conductor.

### 3.2.2 Axial Grading

In axial grading, the axial component of the electric field  $E_z$  is kept constant between all of the foils. The following equations prove that the length of each foil must decay by a constant value for each consecutive foil, and the radius at which it is placed is determined by a simple iterative formula.

The axial electric field is related to the voltage difference and the length change between each consecutive foil as in equation 9. Under symmetric capacitive grading,  $b_n = b_{ln} = b_{rn}$  with reference to figure 3.4.  $\Delta V$  is already defined as a constant from equation 3, and so to have equal field, the change in foil length  $b_n$  should also be constant.

$$E_z = \frac{\Delta V}{b_n} = \text{Constant} \quad (9)$$

The relationship between  $L_n$  and  $b_n$  is defined in figure 3.4, as explained in equation 10.

$$L_n = L_{n-1} - 2b_n \quad (10)$$

Since equation 9 requires the change in foil length  $b_n$  to be constant, equation 2 for coaxial capacitance requires the radius of each foil to change from foil to foil. This can be simplified to a similar form as equation 6, except that the initial information required, in this case, is different. The necessary parameters are: the length of the first foil( $L_1$ ), the radius of conductor and first foil( $r_0, r_1$ ). However, for initial calculation of  $L_n$ ( $n = 1, 2, \dots, N$ ) the size of the constant difference in length between each of the foils should be known ( $b_n$ ). All other lengths and radii can then be calculated.

In case of axial grading where different material is used on each side of the bushing ( $b_{ln} \neq b_{rn}$ ), a similar calculation is carried out for each side. The total length of each foil is found by adding  $L_{ln}$  and  $L_{rn}$ . Furthermore, position of each foil could be calculated using the recursive formula in equation 11

$$r_n = r_{(n-1)} \exp \left( \frac{L_n}{L_1} \ln \left( \frac{r_1}{r_0} \right) \right) \quad (11)$$

## 4 Design Details

The reference model for this project is shown in figure 4.1. The reference design is a paper impregnated with oil bushing with 21 aluminium foils of  $100\mu\text{m}$  thickness. One side of the bushing is exposed to air, the other to oil, similar to a transformer bushing. The diameter of the conductor is 100mm, the bushing diameter is 300mm. The length of the first foil is 5000mm long, and fixed 2mm into the bushing at the conductor voltage. The outer foil is also set 2mm inside the bushing and is directly connected to the earthed flange. The conductor is used at 275kV AC voltage, and the design was taken from a bushing that was in operation for around 30 years.

### 4.1 Design Issues

In section 3.2 the initial information required for both radial and axial grading includes the length and radial displacement of the innermost foil. In the reference design the following initial information is given in table 4.1.

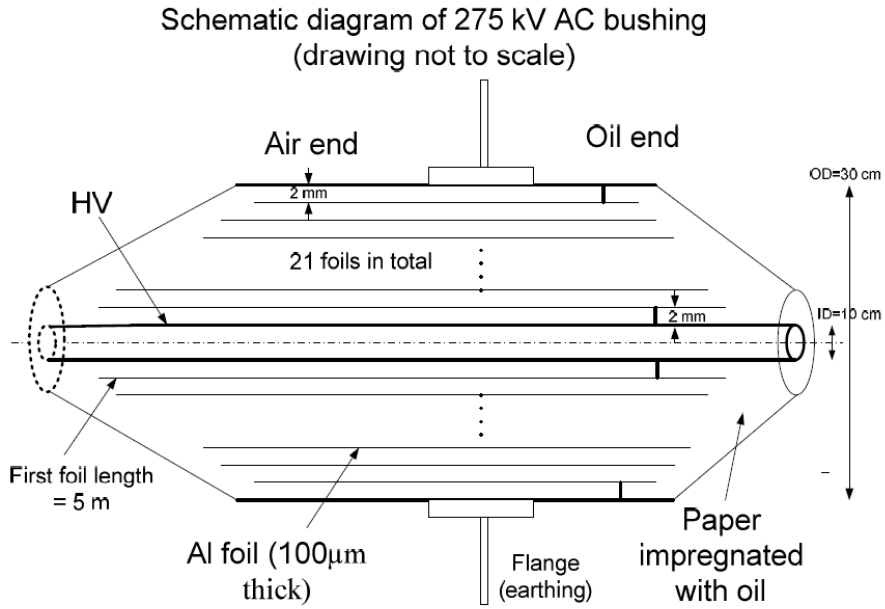


Figure 4.1: The reference problem taken from [16]

Table 4.1: Initial Information for Reference Design

| Initial Information         | Value  |
|-----------------------------|--------|
| Conductor Diameter (ID)     | 100mm  |
| First Foil Length $L_1$     | 5000mm |
| First Foil Radius $r_1$     | 52mm   |
| Outer Bushing Diameter (OD) | 300mm  |
| Outer Foil Radius $r_{21}$  | 148mm  |

This information intuitively fits radial grading best, since there is no requirement to assume the length of the outermost foil. However, there is a discrepancy between the standard literature problem and the reference design. The first foil is connected to the high voltage conductor, and the last foil is connected to the earthed flange. This is to eliminate the electric field on the boundary interface as far as possible on both sides of the bushing, so that the voltage drop occurs exclusively inside the bushing insulation.

This has an impact on the calculations described in section 3.2. Since the innermost foil is at the same voltage as the conductor, there is no capacitance between them, as shown in figure 4.2. The derivation of the iterative equations assumes a capacitance between the current foil and the previous foil or conductor ( $r_n, r_{n-1}$ ). The first foil in figure 4.1 is therefore indexed as 0 and not 1.

This means that there is not sufficient initial information to proceed with either radial or axial grading, since the first non-connected foil length  $L_1$  is not given. The iterative equations require the first non-connected foil length  $L_1$  for radial ( $L_1$  &  $r_1$  for axial) grading to be known as shown in equation 12 and 13. In the radial grading case, all radii variables are known due to the even spacings under radial grading. In the axial grading case, the length of foils are known due to known parameters  $b_{ln}$  and  $b_{rn}$ .

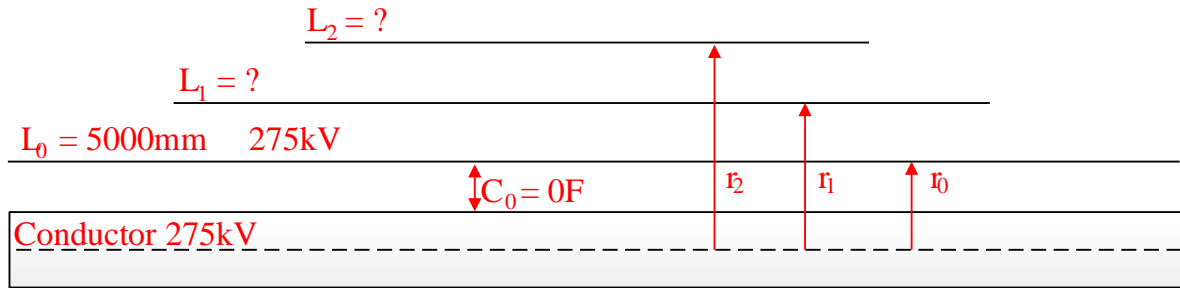


Figure 4.2: Diagram to explain the assumptions required

$$L_2 = L_1 \frac{\ln\left(\frac{r_2}{r_1}\right)}{\ln\left(\frac{r_1}{r_0}\right)} \quad (\text{Radial grading}) \quad (12)$$

$$r_2 = r_1 \exp\left(\frac{L_2}{L_1} \ln\left(\frac{r_1}{r_0}\right)\right) \quad (\text{Axial grading}) \quad (13)$$

If this is not taken into account then a flawed design will be produced in both cases. Equations 14 and 15 show a wrongly described first iteration of the radial and axial grading formula. For radial grading the resulted design is shown in figure 4.3. This shows that the length of second foil is much bigger than the first foil. This is clearly wrong, and does not give the hyperbolic shape from the beginning of the foils.

$$L_1 = 5000 \frac{\ln\left(\frac{56.8}{52}\right)}{\ln\left(\frac{52}{50}\right)} = 11256\text{mm} \quad (\text{Radial grading}) \quad (14)$$

$$r_2 = 52 \exp\left(\frac{49418}{5000} \ln\left(\frac{52}{50}\right)\right) = 54.05\text{mm} \implies r_{21} = 103.52\text{mm} \quad (\text{Axial grading}) \quad (15)$$

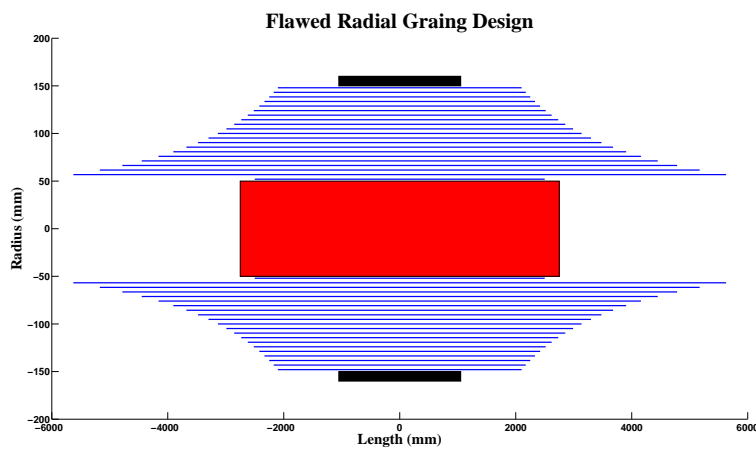


Figure 4.3: Flawed Radial Grading Design

In order to proceed with the calculations there must be an assumption of the length of the first unconnected foil. A reasonable assumption is that this follows the hyperbolic shape of the other foils in radial grading. In axial grading the foil lengths are expected to decay with the axial field strength.

Both of these expectations are realised when the first foil is assumed to be isolated for calculation purposes only. These assumptions in both cases help to evenly distribute the electric field radially or axially accordingly. To achieve this design mathematically, the following assumptions are made for the calculations only:

1. Foil 0 is not connected to the HV conductor for both cases.
2. The conductor surface is spaced a distance of  $S_n$  from foil 0 in **radial grading**.
3. The conductor surface is spaced an adjustable distance from foil 0 in **axial grading**.

The reason of each assumption according to the design constrains are explained as following:

- Assumption 1 is required to be able to use the capacitor derived iterative formula on foil 0.
- Assumption 2 is required so that the radial spacing is kept constant.
- Assumption 3 is required so that axial grading could be calculated with a varying parameter value for  $r_0$ . This makes it possible to adjust the initial gap so that the last foil will be placed exactly at 148mm.

The first iteration has been calculated under these assumptions, giving the result in equations 16 and 17 which are expected values. The remainder of foil parameters can then be calculated using the iterative formulas in each grading.

$$L_1 = 5000 \frac{\ln\left(\frac{56.8}{52}\right)}{\ln\left(\frac{52}{47.2}\right)} = 4558mm \quad (\text{Radial grading}) \quad (16)$$

$$r_2 = 52 \exp\left(\frac{49418}{5000} \ln\left(\frac{52}{50 - 1.007}\right)\right) = 55.15mm \implies r_{21} \simeq 148mm \quad (\text{Axial grading}) \quad (17)$$

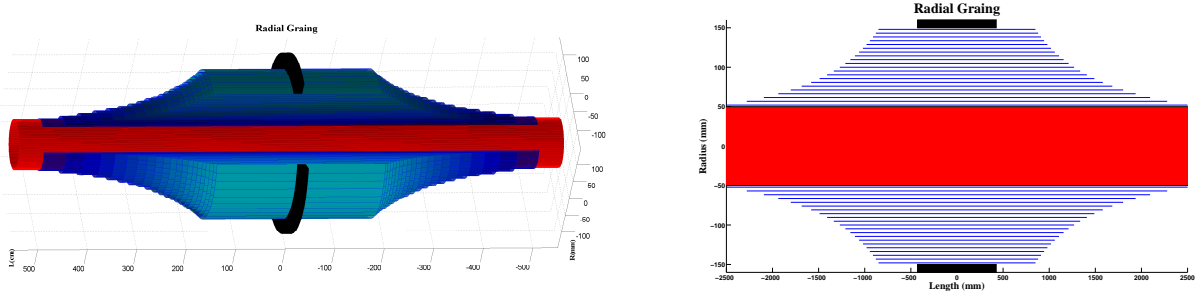
## 5 Matlab Calculations

Two Matlab scripts were developed for computation of radial and axial grading. These scripts were built to be easily customisable for any number of foils and any initial values, to cater for the calculation of improved designs. They also automatically output data in a form for direct input into the COMSOL model, auto-update a L<sup>A</sup>T<sub>E</sub>Xfile containing the data to form results table and displays the results in both 2D and 3D plots for quick design verification.

### 5.1 Matlab Radial Grading

In the case of radial grading the code takes a required number of foils, and the inner and outer dimensions of the bushing, to calculate the radial location and length of each foil using the radial grading method as described in section 3.2 and also using the assumptions made for radial grading design on 4.1.

For current design with specified parameters, the script plots the calculated foil positions in a 3D graph shown in figure 5.1. Also the 2D plot of this design is shown in figure 5.1(b). This figure



(a) 3D Representation of foil radial position and length

(b) 2D Representation of foil radial position and length

Figure 5.1: Matlab Generated Plots of Geometric Radial Design

illustrates the hyperbolic shape which was expected for radial grading. These figures allows a quick verification of the scripts accuracy before proceeding to simulation.

Table 5.1 shows the values obtained for radial grading.

| Foil N.O | Radius(mm) | Length(mm) | Foil N.O | Radius(mm) | Length(mm) |
|----------|------------|------------|----------|------------|------------|
| 1        | 52.00      | 5000.00    | 12       | 104.80     | 2420.43    |
| 2        | 56.80      | 4558.22    | 13       | 109.60     | 2312.01    |
| 3        | 61.60      | 4188.21    | 14       | 114.40     | 2212.90    |
| 4        | 66.40      | 3873.79    | 15       | 119.20     | 2121.93    |
| 5        | 71.20      | 3603.30    | 16       | 124.00     | 2038.15    |
| 6        | 76.00      | 3368.13    | 17       | 128.80     | 1960.73    |
| 7        | 80.80      | 3161.78    | 18       | 133.60     | 1888.98    |
| 8        | 85.60      | 2979.27    | 19       | 138.40     | 1822.29    |
| 9        | 90.40      | 2816.68    | 20       | 143.20     | 1760.16    |
| 10       | 95.20      | 2670.92    | 21       | 148.00     | 1702.12    |
| 11       | 100.00     | 2539.51    | 22       | 150.00     | 0.00       |

Table 5.1: Radial Grading Calculations Results

## 5.2 Matlab Axial Grading

The axial grading script is similar to the radial grading script in design. However, as it is explain in reference [15], the constant difference of foil length in oil and air side of bushing ( $b_{air}$ ,  $b_{oil}$ ) is calculated by considering the value of flash over distance  $L_{air}$  and  $L_{oil}$ . These values are calculated by using the fact that average electric field strength along the boundary surface in oil side should be 3 to 4 Kv/cm and nearly 9 to 12 Kv/cm in air side of the bushing. These values are calculated using equation 18.

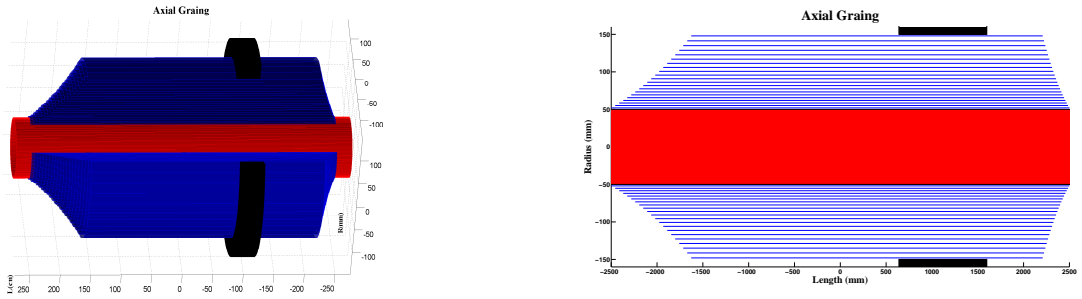
$$b_{air} = \frac{\Delta V}{900 \text{ v/mm}} \quad b_{oil} = \frac{\Delta V}{300 \text{ v/mm}} \quad (18)$$

Additionally, as shown in equation 19, in the calculation of  $r_2$  a parameter called  $R_{parameter}$  is subtracted from  $r_0$  to change the position of assumed conductor surface. The radius of the last foil ( $r_{21}$ ) could be correctly adjusted by making changes in this parameter and executing the script.

$R_{parameter} = 1.007\text{mm}$  was the best value found for this design.

$$r_2 = r_1 \exp\left(\frac{L_2}{L_1} \ln\left(\frac{r_1}{r_0 - R_{parameter}}\right)\right) \quad (19)$$

The script plots 2D and 3D plots of axial grading to the user. Figure 5.2(a) illustrates the 3D configuration of the design's axial bushing. The 2D plot of this design, which is shown in figure 5.2(b), shows a nearly straight line from the edges of the first to last foil. In fact, the foil length reduction is constant on both sides ( $b_{oil}, b_{air}$ ). But, as the Matlab script is using the exact calculation (non-linear) rather than the approximate method (linear), the foil endings are not placed exactly on a straight line. It also illustrates that  $b_{air} > b_{oil}$  as it was expected due to the relative permittivity of each material. Finally the calculated values for axial grading, using this design method, are shown in 5.2. These values along the given parameters in table 5.3 were used for COMSOL simulations of this axial grading design.



(a) 3D Representation of foil radial position and length

(b) 2D Representation of foil radial position and length

Figure 5.2: Matlab Generated Plots of Geometric Axial Design

| Foil N.O | Radius(mm) | Length(mm) | Foil N.O | Radius(mm) | Length(mm) |
|----------|------------|------------|----------|------------|------------|
| 1        | 52.00      | 5000.00    | 12       | 95.65      | 4359.84    |
| 2        | 55.15      | 4941.80    | 13       | 100.68     | 4301.64    |
| 3        | 58.46      | 4883.61    | 14       | 105.90     | 4243.44    |
| 4        | 61.92      | 4825.41    | 15       | 111.32     | 4185.25    |
| 5        | 65.53      | 4767.21    | 16       | 116.93     | 4127.05    |
| 6        | 69.32      | 4709.02    | 17       | 122.73     | 4068.85    |
| 7        | 73.26      | 4650.82    | 18       | 128.74     | 4010.66    |
| 8        | 77.39      | 4592.62    | 19       | 134.95     | 3952.46    |
| 9        | 81.68      | 4534.43    | 20       | 141.35     | 3894.26    |
| 10       | 86.15      | 4476.23    | 21       | 147.96     | 3836.07    |
| 11       | 90.81      | 4418.03    | 22       | 149.96     | 0.00       |

Table 5.2: Axial Grading Calculations Results

The final information required to be able to proceed to the simulation phase is the relative permittivity of each material. This was gathered from [13] and is shown in table 5.3. This data is used in all COMSOL models.

| Material                   | Relative Permittivity ( $\epsilon_r$ ) |
|----------------------------|--|
| Air                        | 1                                      |
| Oil                        | 2.2                                    |
| Paper Impregnated with Oil | 4                                      |
| Aluminium                  | $10^8$                                 |

Table 5.3: Relative Permittivity of Materials

## 6 Modelling Results

The following simulations were completed using the COMSOL multiphysics software package. COMSOL is a professional finite element simulation package able to model a variety of physical features. The following models are created using the AC/DC module, which is used to simulate electric and magnetic fields [17]. Specifically, the electrostatics interface is used. This solves a charge conservation equation for a given voltage and spacial distribution of charge [17].

### 6.1 Finite Element Methods (FEM)

There are inherent difficulties in solving the partial differential equations that govern many practical engineering problems [4]. Despite knowing the equations and appropriate boundary conditions that govern a problem, many are complicated by irregular geometries or other discontinuities. Numerical methods allow approximate solutions to be obtained for problems intractable by analytic methods [18]. In an analytic solution, the whole system is governed by a mathematical equation valid for the entire region of interest. Although these differential equations are often mathematically compact, it is difficult to obtain an answer unless the system is unreasonably simplified [18]. In FEMs, the complex geometry is broken into a series of much smaller and simpler geometries [4]. These geometries can be squares, rectangles or triangles in 2D or the 3D equivalent shapes. These simpler shapes form interconnected subregions for which an approximate function, usually a high order polynomial, can be used to represent the actual function. If the complex geometry is split into an adequate number of simple shapes, these approximate functions closely matches the exact solution [18].

By default COMSOL uses a triangular discretisation to split up a complex geometry in a process called meshing. This forms an unstructured grid of triangles, allowing the mapping of complex or curved geometries. Other numerical methods such as Finite Difference Methods require a structured grid, hence FEMs are more flexible with regards to geometry [4]. Meshing requires an initial understanding of the expected outcomes of the problem, so that the mesh can be refined in areas of interest. Each triangular element is approximated by a linear interpolation of the potential at the vertices of the triangle. A set of linear algebraic equations are formed by minimising the error between the actual solution and a set of approximate linear trial functions [18].

### 6.2 Equation Derivation and Boundary Conditions

The electrostatics interface of the AC/DC COMSOL module uses the electric potential  $V$  to calculate static electric fields. A Poisson type partial differential equation is derived using classical electrostatics and Gauss' Law [19].

By taking Gauss's Law:

$$\nabla \cdot \mathbf{D} = \rho v \quad (20)$$

the equation for electric flux density  $\mathbf{D}$ :

$$\mathbf{D} = \epsilon_0 \epsilon_r \mathbf{E} \quad (21)$$

this can be combined with the equation for a static electric field:

$$\mathbf{E} = -\nabla V \quad (22)$$

to give by substitution:

$$\nabla \cdot \mathbf{D} = \nabla \cdot (\epsilon_0 \epsilon_r \mathbf{E}) = -\nabla \cdot (\epsilon_0 \epsilon_r \nabla V) = \rho v \quad (23)$$

which is more usually written:

$$\nabla^2 V = -\frac{\rho v}{\epsilon_0 \epsilon_r} \quad (24)$$

where  $\epsilon_0$  is the permittivity of free space,  $\epsilon_r$  is the relative permittivity of the material,  $\mathbf{E}$  is the electric field strength and  $\rho v$  is the volume charge density.

In the special case where there is zero volume charge density, that is  $\rho v = 0$  then the equation simplifies to Laplace's Equation:

$$\nabla^2 V = 0 \quad (25)$$

The models used in this paper are 2D axisymmetric, meaning that a 2D model is used to describe a 3D object that can be rotated  $360^\circ$  about a central point  $r = 0$  to give a 3D geometry. This assumes that not only is the geometry the same in the angular  $\varphi$  direction, but also that the electric potential is constant. In this case, Poissons equation can be rewritten in cylindrical coordinates for a 2D axisymmetric model, it is multiplied by  $r$  to ensure there are no singularities at  $r = 0$  [18].

$$\begin{bmatrix} \frac{\partial}{\partial r} \\ \frac{\partial}{\partial z} \end{bmatrix}^T \cdot (r \begin{bmatrix} \frac{\partial V}{\partial r} \\ \frac{\partial V}{\partial z} \end{bmatrix}) = -\frac{r \rho v}{\epsilon_0 \epsilon_r} \quad (26)$$

The boundary conditions are defined as the following:

1. All boundaries with the conductor and with foil 0 are set to  $V = V_0 = 275kV$
2. All boundaries with the transformer wall and with the outermost foil are set to  $V = 0$
3. The interface between two insulator sub-domains is defined by  $n \cdot (\mathbf{D}_1 - \mathbf{D}_2) = \rho v$  and  $n \times (\mathbf{E}_1 - \mathbf{E}_2) = 0$ . These equations specify that the normal component of the electric flux density is discontinuous at the interface between two dielectrics, and that the tangential component of the electric field is continuous across the dielectric interface.  $n$  is the normal outward vector pointing from dielectric 2 to dielectric 1.

### 6.3 Workflow

In order to simulate the electric field distribution within our bushing design, 2D axisymmetric models were created. The general workflow to achieve this is:

1. Build a geometry representing the physical structure of the bushing.

2. Assign each geometric domain a material. The material selection determines the relative permittivity  $\epsilon_r$  of each domain.
3. Define the charge conservation equation and all initial conditions. This includes setting which boundaries are at ground and conductor potential and setting boundary conditions.
4. Design a mesh. The geometry is split into smaller elements in order to compute the charge conservation equation. For designs with foils, special meshing parameters are required to speed up the process.
5. Carry out the study. This stage is the actual computation of the solution.
6. Post-processing. Display the results in a number of formats including 3D, 2D and 1D plots, or export the data for post-processing in Matlab.

#### 6.4 Baseline Model

In order to minimise the computation time required for each model, it was necessary to determine the areas of interest in the model. A bushing geometry was built with no foils inserted. A high quality mesh was produced and the system was solved to find the electric field distribution throughout the bushing and the surrounding area.

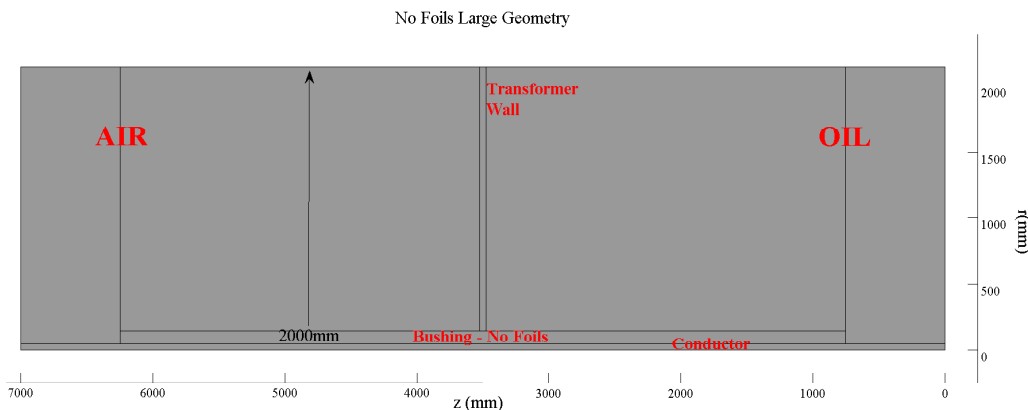


Figure 6.1: Baseline Model Geometry

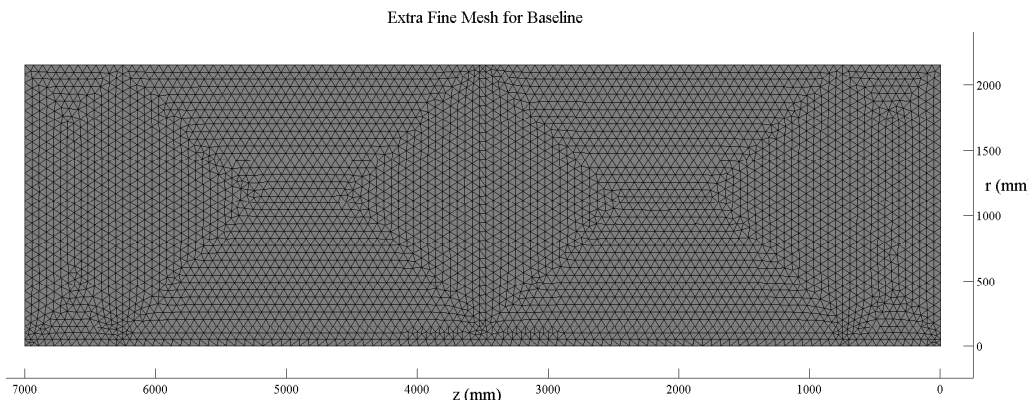


Figure 6.2: Extra Fine Meshing for Baseline Model

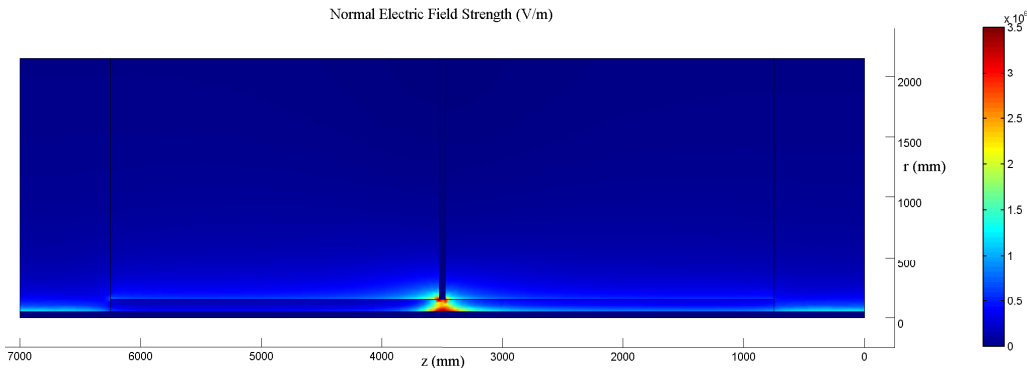


Figure 6.3: Normal Electric Field (V/m) for Baseline Model

The air and oil extends radially 2m from the end of the bushing and 1m in the axial direction. This is to understand the anticipated area of interest in the model. By considering figure 6.3 it is clear that there is very little happening further than 500mm radially from the bushing surface and there is very little of interest further than 200mm in the axial direction. Therefore all further models will adhere to this geometry, ensuring that the area of interest is captured, while decreasing simulation times to a minimum.

In figure 6.3, the normal electric field throughout the whole system is displayed. Electric field is usually taken to be a vector quantity, that is a magnitude and direction. For example, the electric field in the radial direction is termed  $E_r$  and in the axial direction is  $E_z$ . The normal electric field is not a normal vector, but an absolute value of the electric field strength at a given point. This can be described mathematically as  $normE = \sqrt{\mathbf{E} \cdot \mathbf{E}}$ . It gives a reasonable interpretation of the electric field strength in either vector direction in the model, and will be used to compare all other models.

## 6.5 No Foils

In order to illustrate the requirement for capacitive grading within AC bushings, a simulation of a bushing with no foils was conducted. Figure 6.4 shows the geometry and materials used for each section. The conductor length is 6000mm and has a width of half the inner diameter, 50mm. The paper impregnated with oil insulation is 5500mm long in order to accommodate the first foil length of 5000mm with sufficient clearance. The transformer wall is modelled as a 50mm high aluminium block that is 500mm wide, and is placed vertically in the middle of the design. The surrounding oil and air are 500mm wide at the centre of the bushing, and extend to the length of the conductor. The paper impregnated with oil insulation is sloped to avoid sharp corners and high field strengths.

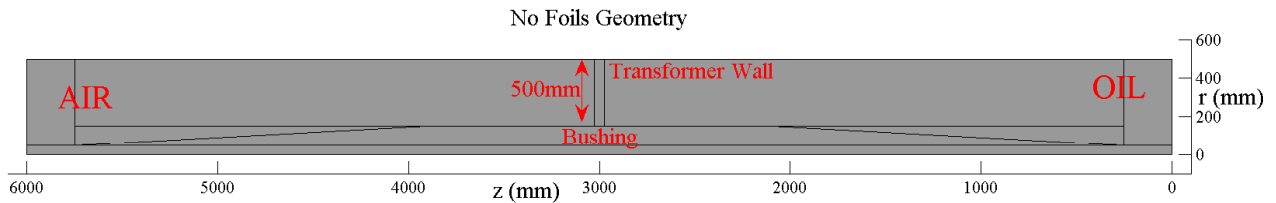


Figure 6.4: Geometry and Materials for No Foils Bushing

A very fine mesh was used in this model as shown in figure 6.5. This allows for the maximum level of accuracy in the results produced, and is possible since the geometry of this model is not over-complex.

It was necessary to ensure the mesh in the plane of the transformer wall was very fine in order to sufficiently capture areas of very high field.

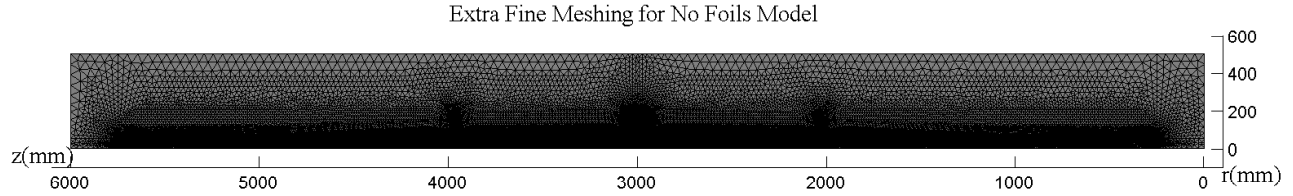


Figure 6.5: Extra Fine Mesh for No Foils Bushing

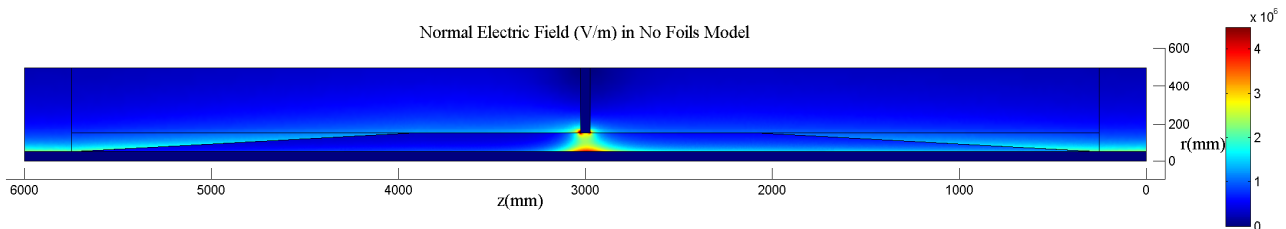


Figure 6.6: Normal Electric Field (V/m) for No Foils Bushing

The motivation for capacitive grading is clear in figure 6.6. The central area of stress in the plane of the transformer wall is shown in figure 6.7. The highest stress is shown at the corners of the transformer wall and in the plane between the transformer wall and the conductor. This reaches field strengths greater than  $4.5\text{kV/mm}$  which can cause the inception of partial discharge. This simulation bears close resemblance to figure 3.1 in section 3 of this report, which was used to describe the electric field problem. In order for this bushing to function within the design constraints, capacitive grading must be used.

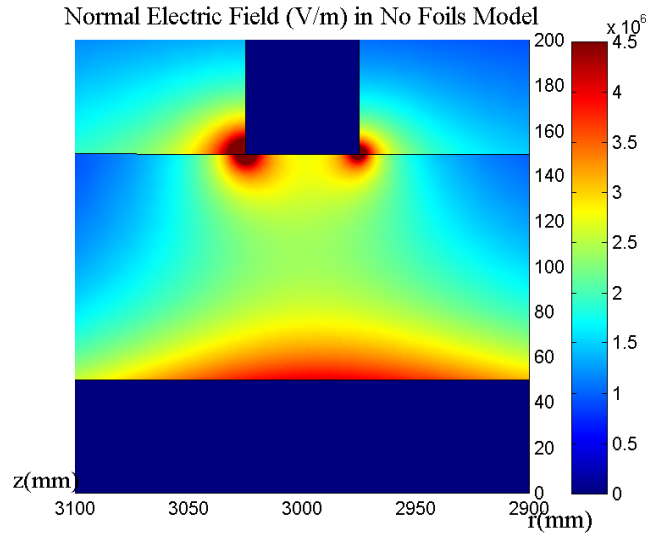


Figure 6.7: Area of very high electric stress

## 6.6 No Grading

In order to rectify the high electric stress identified in the no foils model, isolated foils are introduced to capacitively grade the electric field. To prove the requirement for grading the lengths or radial

displacement of the foils, a simulation where the foils are maintained at the same length was performed. This model was expected to fail the design criteria, proving that introducing isolated foils into the bushing achieves very little and it is the radial or axial grading of the field that is critical. The bushing has 21 foils spaced at an even radial spacing, but with no change in length of each foil. Each foil is 1756mm in length, and is centred in the within the bushing.

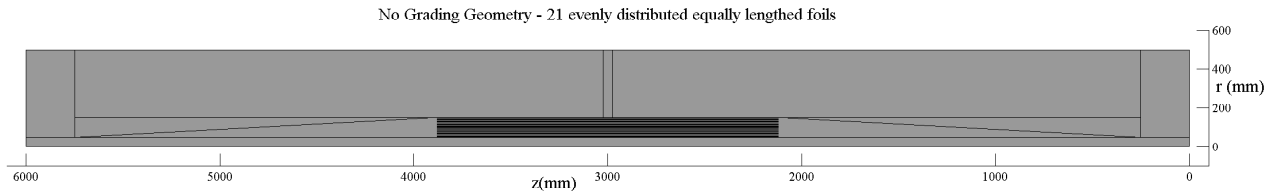


Figure 6.8: Geometry of the No Grading Model

Producing a finite element mesh for this model caused issues with long computation time. Even using the coarsest default setting, the meshing time was of the order of days. This is due to the difference in size of the aspects of the geometry. The foils are just 0.1mm thick, which requires a very small set of triangles in order to mesh this area. The other domains are up to 6000mm long, which is considerably larger and requires a different size of triangles.

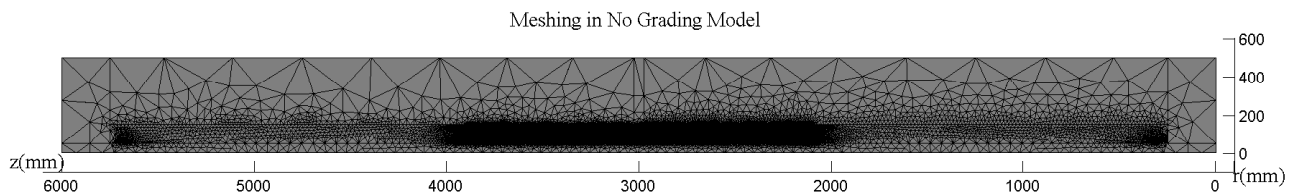


Figure 6.9: User defined meshing for no grading simulation - whole view

In order to solve the issue, a set of meshing rules were produced. Firstly, the mesh within the conductor and within the foils can be very coarse. Within a conducting material, no electric field is expected, hence there is no reason to finely mesh that area. Areas of interest or areas where the field changes rapidly need to have a very fine mesh to ensure the accuracy of the results is sufficient. The meshing rules dictated a minimum number of points at the tip of each foil, and along the surface of the bushing. This resulted in a refined mesh shown in figures 6.9 and 6.10.

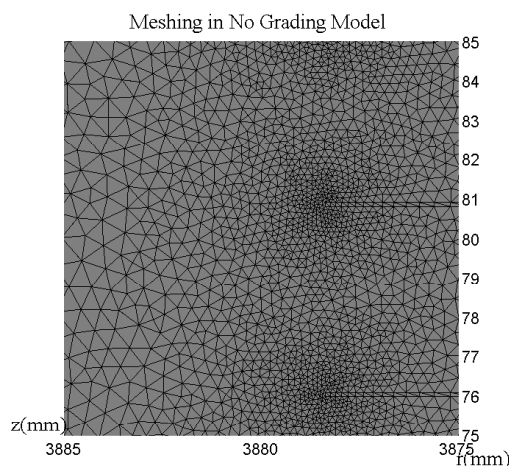


Figure 6.10: User defined meshing for no grading simulation - foil tip view

Once the geometry has been meshed appropriately, the system can be solved to determine the electric field strength throughout the model, as shown in figure 6.11.

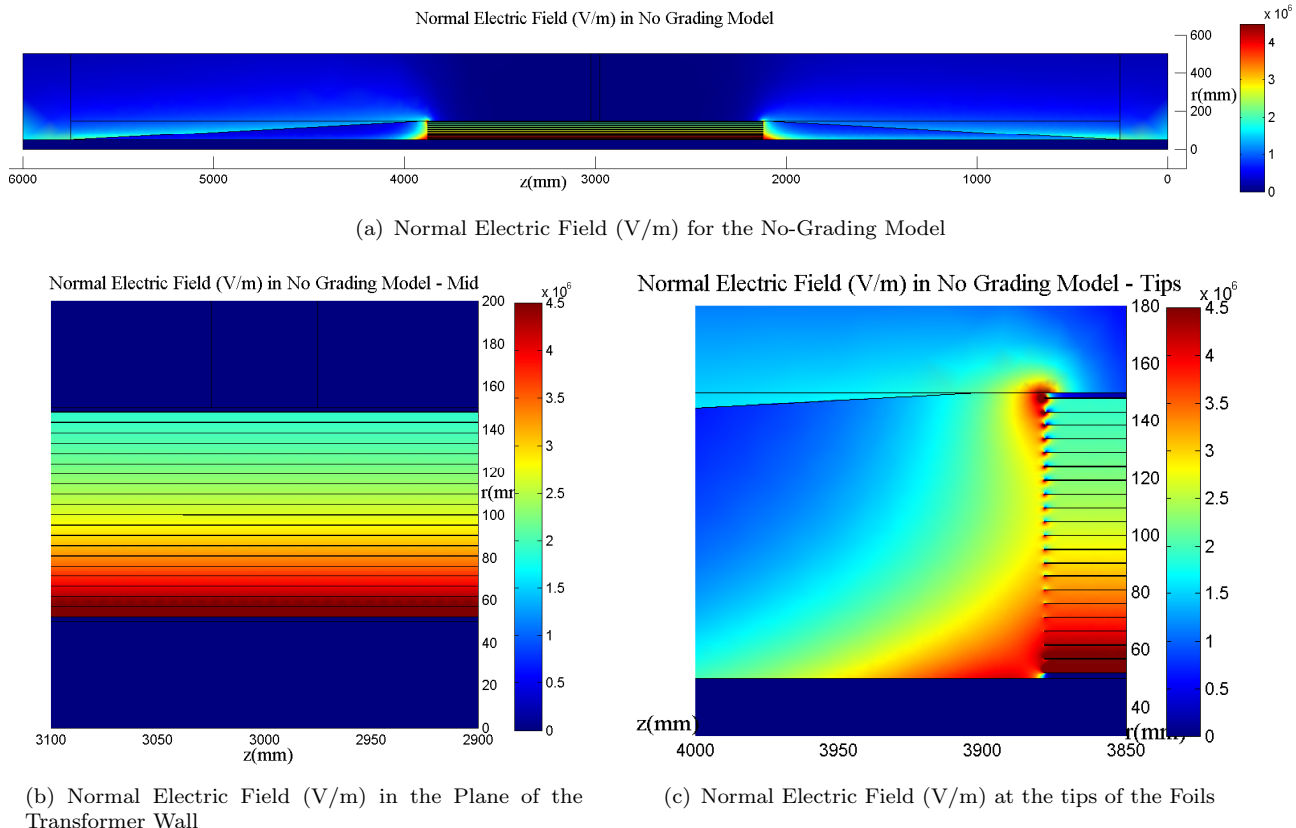


Figure 6.11: Examination of the Electric Field in the Non-Grading Model

Figure 6.11(b) shows the normal electric field in the plane of the transformer wall. The areas of very high field at the corners of the transformer wall have been eliminated by the use of the capacitive foils. However, the field close to the conductor is still very high. An additional issue is introduced by using capacitive foils. Considering figure 6.11(c), the tips of the foils cause some considerable disturbance of the electric field. This model achieves very little improvement, if at all, over the model with no foils.

Now that the requirement for grading has been shown in section 6.6, and the requirement to use a formal axial or radial grading method in this section, the radial and axial designs can be compared.

## 6.7 Radial Grading

The COMSOL geometry for the radial grading model is shown figure 6.12. Each foil is an equal radial distance according to the radial grading method. The lengths of each foil are taken from table 5.1. The remainder of the geometry is identical to the No Foils and No Grading models.

As with the No Grading model, the geometry in this design is very complex with a variety of scales. In order to reduce computation time but maintain a reasonable level of accuracy in areas of interest, the mesh was produced to the rules outlined for the No Grading model. The meshing for this model is shown in figure 6.13 and 6.14.

The model was then solved to find the normal electric field throughout the model. It can be seen in figure 6.21(a) that the field between the foils nearest the conductor is reduced below  $4.5 \text{ kV/mm}$ . This

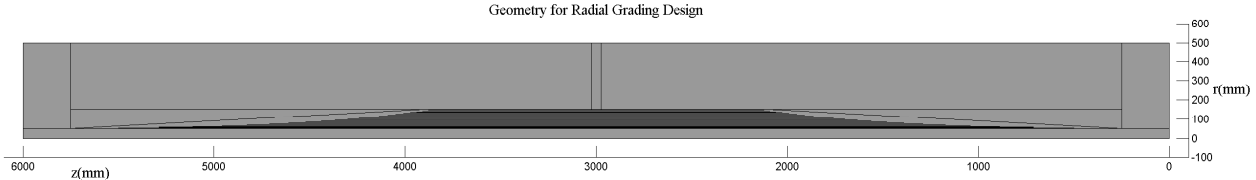


Figure 6.12: Geometry of the Radial Model

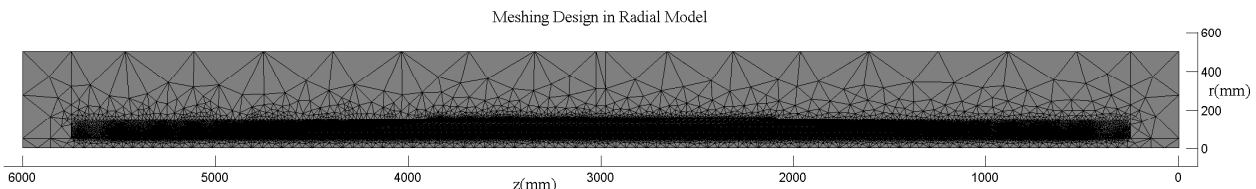


Figure 6.13: Meshing of the Radial Model

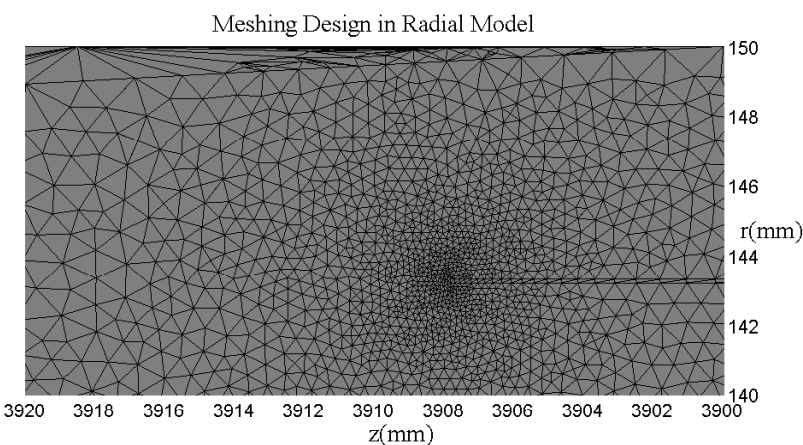


Figure 6.14: Meshing of the Radial Model Focused on a Foil Tip

is now evenly spread in the radial direction, as expected due to the radial grading of the electric field. The electric field in the radial direction is much improved.

However, the axial electric field is not considered in the radial grading design method. The field at the foil tips is largely due to the axial field strength. It is necessary to inspect the strength of the electric fields at the tips of the foils. It can be seen in figure 6.21(b) that the electric field at the tips of the foil exceeds  $4.5\text{kV/mm}$  in some places. Section 7 will take this observation further, to establish if it meets the design criteria.

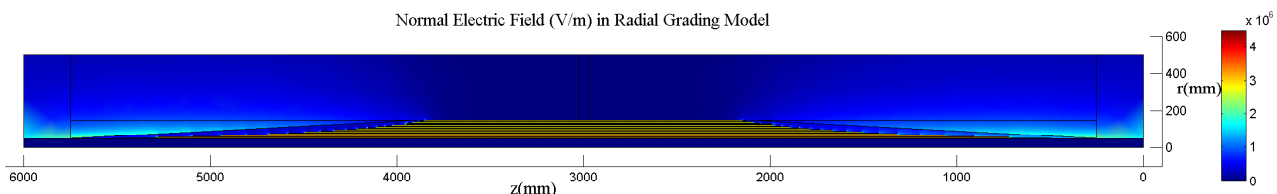
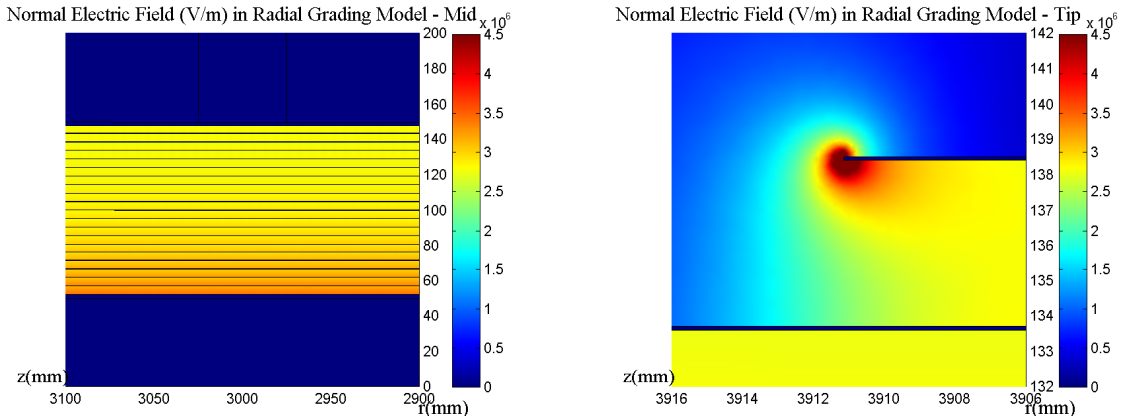


Figure 6.15: Normal Electric Field (V/m) for the Radial - Whole view



(a) Normal Electric Field (V/m) in the Plane of the Transformer Wall      (b) Normal Electric Field (V/m) at the tips of the Foils

Figure 6.16: Examination of the Electric Field in the Radial Model

## 6.8 Axial Grading

The asymmetric axial grading method results in an uneven geometry about the centre of the bushing. The lengths of each foil is determined in table 5.2. This requires the paper insulation to take a different profile than the other models in order to adequately cover the foils, as shown in figure 6.17. The air side has a much longer surface area due to the higher creepage distance of air.

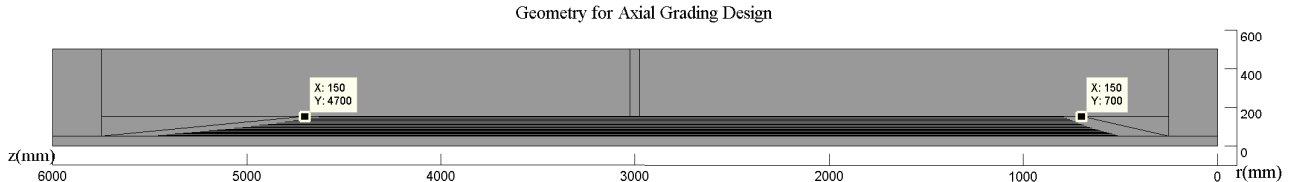


Figure 6.17: Geometry of the Axial Model

The meshing for this model follows the design rules, in order to produce the finest mesh over the key points of interest, shown in figure 6.18. Particularly figure 6.19 shows the fine mesh around the tip and surface of a foil, which is a key area of interest to determine if the PD inception condition is maintained.

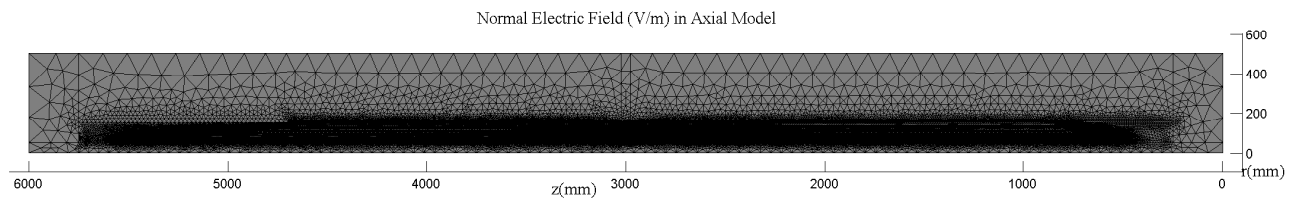


Figure 6.18: Meshing of the Axial Model

The electric field problem can now be solved over the whole model. This produces the surface plots shown in figures 6.20 and 6.21. It can be seen that the field in the plane of the transformer wall is not well graded, as it is neglected in the axial design method. The field at the foil tips for which the main contributor is the axial field has a smaller area exposed to high field strengths than the radial

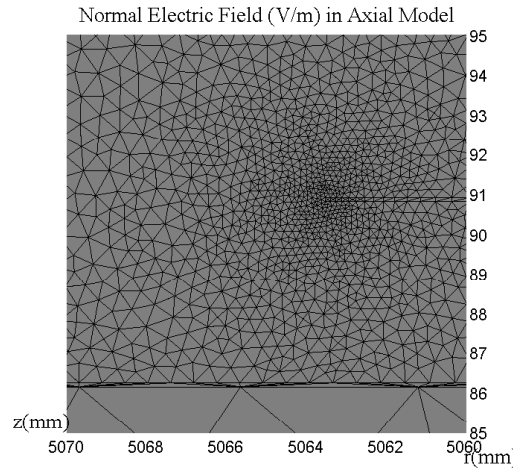


Figure 6.19: Meshing of the Axial Model Focused on a Foil Tip and Surface

method. However, it remains an issue to be considered. This will be discussed and contrasted with the other designs in the discussion in section 7.

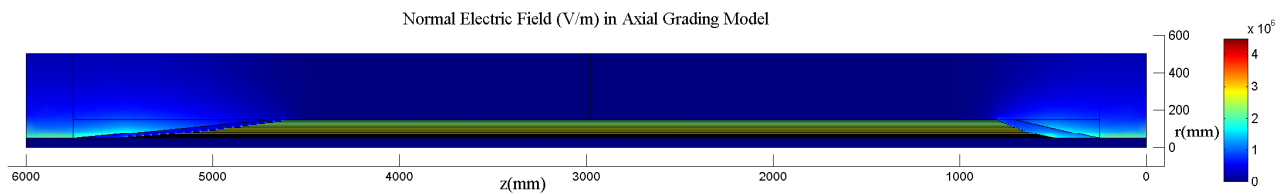
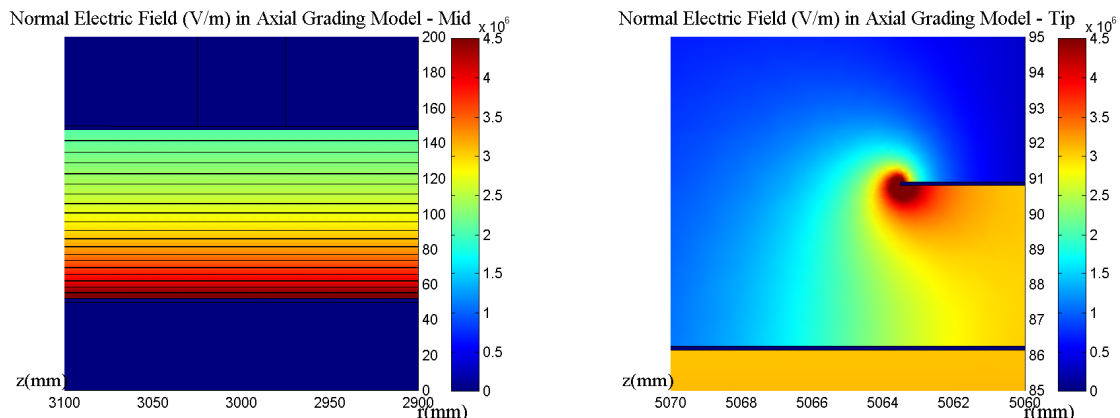


Figure 6.20: Normal Electric Field (V/m) for the Axial Model - Whole view



(a) Normal Electric Field (V/m) in the Plane of the Transformer Wall

(b) Normal Electric Field (V/m) at the tips of the Foils

Figure 6.21: Examination of the Electric Field in the Axial Model

## 7 Discussion

As has been outlined in this report so far, there are problems inherent within bushing design and multiple solutions to these problems. A full discussion and comparison will be made to determine the most accurate and reliable model for HV bushing design. Additionally, reasoning and justification for the incremental changes will outline the development of bushing and possible further improvements that could be made in design.

### 7.1 Success Criteria

In section 2 four criteria were mentioned to determine the efficacy of the design: general/intrinsic breakdown defined by the radial field, surface discharge defined by the axial field, partial discharge within the material defined by areas of high tangential field and corona discharge within air.

Regarding general breakdown it is the largest breakdown strength of the model and so the least likely to fail. High Voltage Engineering Fundamentals has it defined as well in excess of 1MV/cm [4]. The area of interest for this intrinsic breakdown is the line from the conductor straight to the flange, and a measurement of radial electric field.

Surface discharge is not as readily defined for typical graded designs, however a comparison can be made from shedding specifications. Shedding increases the effective creepage length of the bushing by a factor of 4 and for a typical design 40mm/kV is given as the required length for the operational voltage [6]. The IEC 60815 standard defines the creepage distance for ceramic insulators according to levels of pollution in the environment [8]. For bushings less than 300mm in diameter the creepage distance in very heavy pollution levels is 31mm/kV, which is lower than the extreme value quoted in [6]. The creepage distance is multiplied by the highest r.m.s phase-to-phase voltage within the equipment.

Fortunately and reasonably given its significance, partial discharge inception voltage is well defined for all types of insulation material. For resin-impregnated paper the value is 36kV/cm and for oil-impregnated paper the value is 45kV/cm, justifying the more common use of OIP [6]. Due to its nature, a simple investigation of trends is not sufficient to estimate areas of possible PD origins and areas of interest must be found and tested against the inception voltage. They are typically located at the edges of foils or near the conductor itself. If a design passes testing for PD, then it is assumed to pass the intrinsic breakdown requirement since the PD threshold is significantly lower than the intrinsic breakdown threshold.

Corona discharge can occur in both air and oil, however, since the inception voltage is much lower for air and the effects of weather and pollution affect the air side of the bushing much greater it is of higher importance. For the discussion, it will be studied as a subsection of surface discharge.

### 7.2 No Foils

Nowadays, solid bushing is only used for voltages below 25kV. This is due to a combination of all factors as shown in the previous figure 6.6. When simulated with a conductor ten times its rated voltage its flaws are clear. As mentioned previously, the primary criteria to solve are high electric fields inducing partial discharges and large axial fields causing flashover.

This is best illustrated with figure 7.1(b), not only are the fields present at the interface to the flange well in excess of the PD inception voltage, the location of these high electric fields also mean flashover

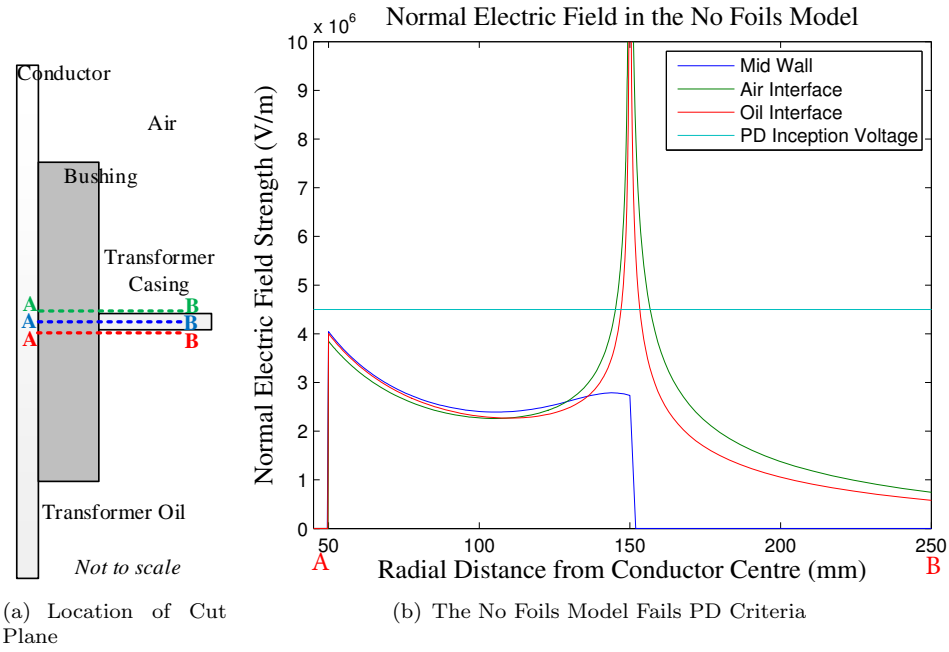


Figure 7.1: The Normal Electric Field in the No Foils Model

is a serious risk due to the lack of shaping of the axial electric field distribution. A result of such localised electric stress is that because the field is greater than the PD inception voltage the voids will generate exponentially more discharges, leading to faster ageing and a much higher chance of breakdown. The solution, assuming keeping voltage constant, would be to increase the bushing height and width.

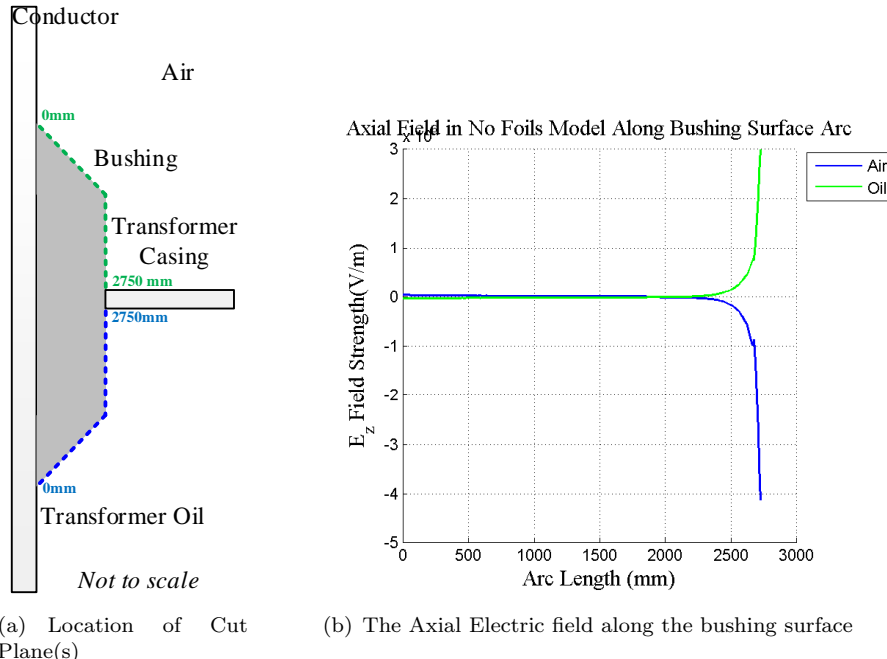


Figure 7.2: Axial electric field along the surface of the bushing

It has already been established that the axial electric field is the primary component for surface discharge. 7.2(b) shows how the axial field varies along the surface of the bushing. Of interest is that

there is very little field throughout the surface apart from at the flange junction; the most sensitive area. The short distances and large fields show that corona discharge is possible and will most likely lead to total failure of the system.

### 7.3 No Grading

The proposal to study a model of condenser bushing without any thought to grading exposes the fundamentals to grading design. Figure 7.3(b) shows that, for the most part the electric field is below the PD inception voltage, at least at the central interface. However looking at figures 6.11(b) and 6.11(c) show that the foil placement did not effectively shape the field at the bushing interface at the tips. Beyond analysing the concentrations of electric field it is important to note that the distribution is non-linear; in comparison to the ideal goal of a linear drop of field across the capacitors [4]. The placement of the outermost foil serves as a location of high field density and although located far from the flange itself it would likely be a source of both PDs and corona discharges.

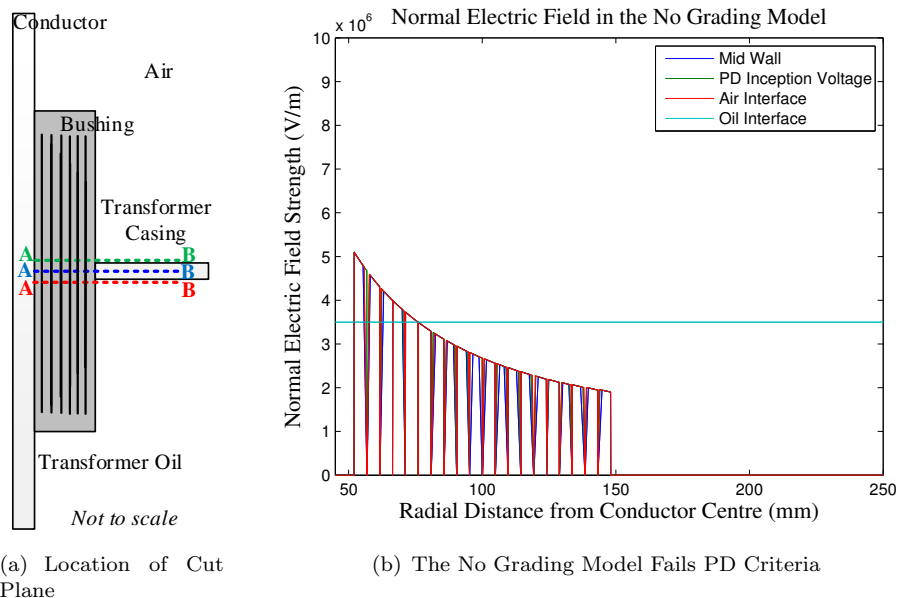


Figure 7.3: The Normal Electric Field in the No Grading Model

The most noticeable change that still displays fault characteristics for the non-graded model is the axial electric field plot along the surface. 6.11(c) is the relevant Electric field plot demonstrating the effect of non-graded foils. Although installing non-graded capacitors did move the large electric fields away from the junction, it clearly failed in reducing the magnitudes of such fields. This is due to a lack of gradient within the foils, allowing a concentration to gather on the edge of the insulation. The resulting effect would be a great deal of PDs and corona discharge and possible surface discharge. The fact that corona discharges not only degrade the medium but lead to a loss of power prove this to be an unsatisfactory and incorrect solution.

One of the goals of capacitive grading, beyond generating uniform fields is to have an electric potential that decreases uniformly from the conductor to flange. The voltage gradient is of course related to electric field and is a possible indicator of bushing performance. However as is shown, the radial electric field through the centre is not of primary concern in regards to testing for failure.

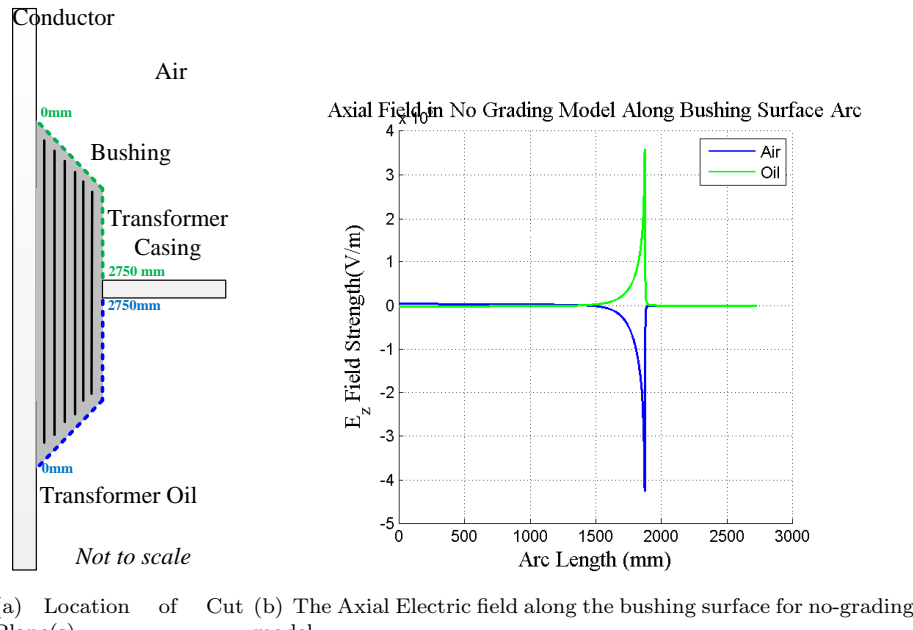


Figure 7.4: Axial electric field along the surface of the bushing

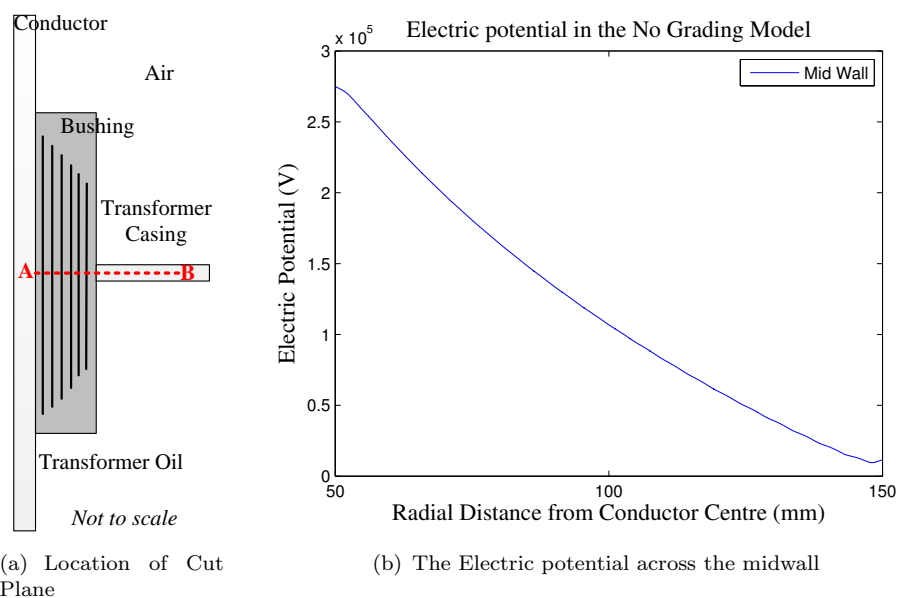


Figure 7.5: The electric potential within the no grading model

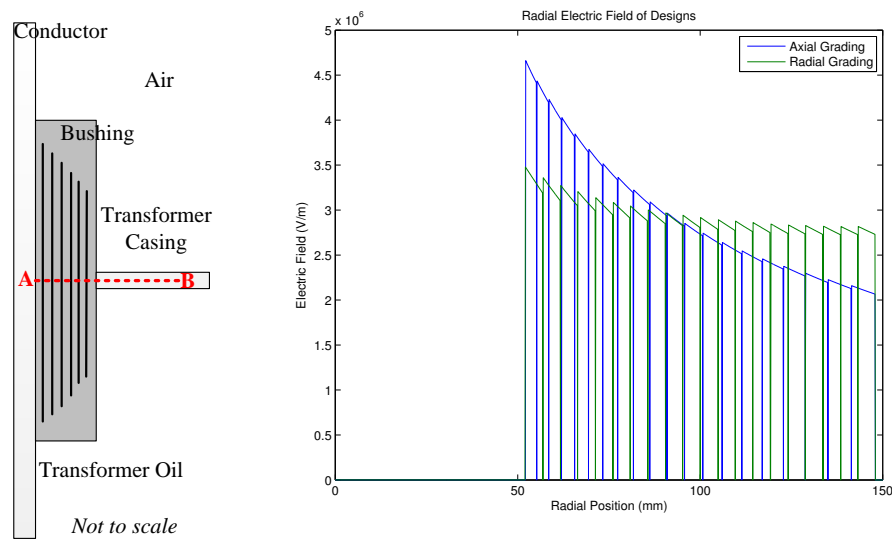
## 7.4 Comparison of Axial and Radial Grading Solutions

The design of both types of capacitive grading method were discussed in the previous sections. The difference in performance of the types in general is the radial grading will improve the intensity of the radial electric field and the axial grading will improve the intensity of the axial electric field. By improvement of intensity of electric field, this means the electric field according to the type of grading method is evenly distributed in a particular direction. Choosing the right design for different application is essential as this will reduce the chances of various types of electrical breakdown and hence the bushing design would be more durable.

There are two components of electric field cause different problems. The radial electric field is mainly responsible to the breakdown of insulating material, for example, electrical breakdown between foils. On the other hand, the axial electric field is mainly responsible to the surface discharges along the boundary of the insulation, for example, corona discharge to the surrounding.

#### 7.4.1 Radial Electric Field

The maximum intensity of the radial electric field for the radial design is expected to be lower than the maximum of the axial design. This means the radial grading design would perform better to suppress the intensity of radial electric field. The radial electric field across the radial direction of both axial and radial grading designs are shown in figure 7.6(b).



(a) Location of Cut (b) Radial electric field across the mid-point of the two designs of bushing.  
Plane

Figure 7.6: The Normal Electric Field compared in the Axial and Radial models

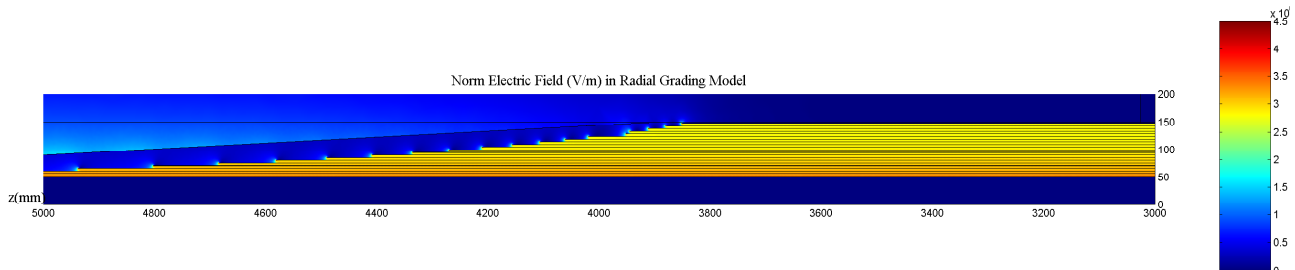


Figure 7.7: 2D surface plot showing the constant distribution of electric field in the axial direction from mid-point to the air end of bushing in the radial design

The result clearly shows the peak value of electric field for the axial design ( $\approx 4.5 \times 10^3 kV m^{-1}$ ) is greater than the peak value of electric field for the radial design ( $\approx 3.5 \times 10^3 kV m^{-1}$ ). Also, from the figure 7.6(b), the radial electric field of the radial grading design is more evenly distributed. This is the effect of grading, hence similar effect should be seen in the axial electric for axial grading design. The electric field distribution across any perpendicular cut lines to the foils would result in almost identical results, because the foils behave similar to capacitors in series. Electric field being constant

across a capacitor and this is true across any two neighbouring foils. Figure 7.7 shows the electric field between consecutive foils from the mid-point to the foil tips. It can be seen that the field is constant in the axial direction between two consecutive foils, except at the tips, which is also true in the axial case.

#### 7.4.2 Axial Electric Field

The axial component of electric field is responsible for the surface discharges along the surface of the bushing design. Axial component of the field contributes to these surfaces, because the axial electric field at the edges of the foil are the most intense. Figure 7.8 shows the magnitude of electric field at each foil edge.

The result shows the axial design has a lower peak value of electric field at these edges of foil. This is the expected result, because axial grading changes the axial field. Also, a clearer maximum peak of electric field should be seen at the outermost foil of the radial graded design due to the sharp turn in the shape of the bushing design. Although the result shows a maximum peak at the last outermost foil, it is not significant. Generally, the electric field at the foil tips in both designs exceeds the partial discharge inception voltage for oil-impregnated paper insulation. This will result in partial discharge.

However, the points which are taken in to consideration are the highest values of electric field locally which drops off rapidly moving away from the point. The sum of the area exceeding the PD threshold is approximately 0.03% of the volume of the overall bushing design, hence, this can be consider as an affordable problem in the bushing design. Also, in the model, all the foils are considered to terminate with a 90° bend. In reality, designs may use various various techniques to suppress the effect of this bend. Some design uses semi-conducting material at the ends of the foil [4].

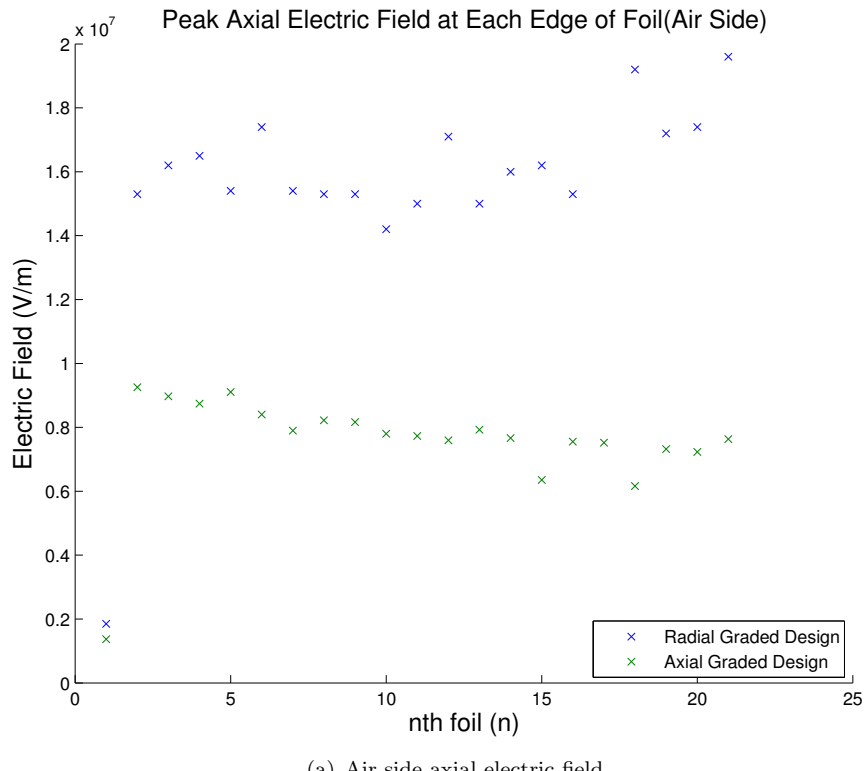
#### 7.4.3 Surface Flashover

Surface flashover is the partial discharge along the surface of the insulation, this is cause by a intense electric field. The parameter which takes into account of surface flashover is the creepage distance as mention previously. The typical value for calculating the creepage distance is 35mm/kV [8]. and for more polluted environment, a higher value of creepage distance might be considered.

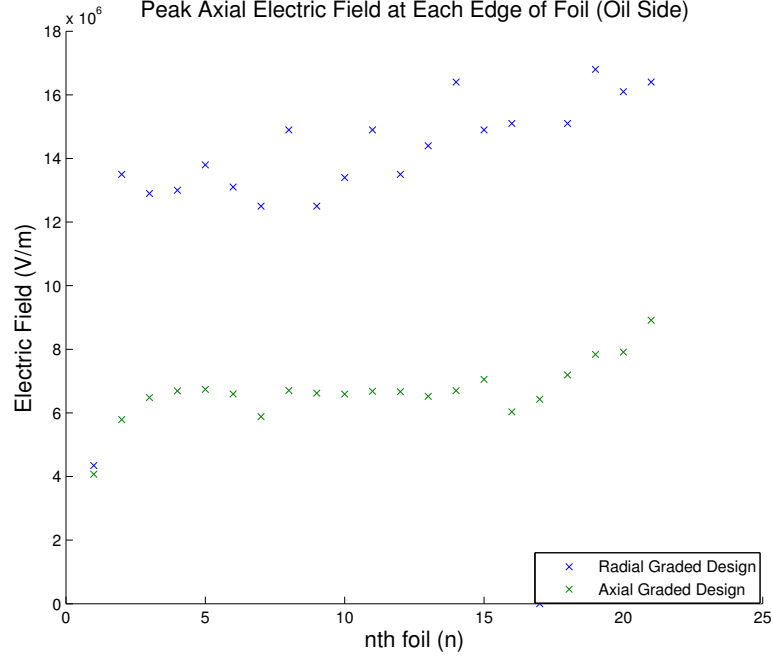
In bushing designs, the creepage distance is increased by the addition of a shed around the bushing. These shed designs increase the creepage distance of insulation designs by increasing the surface length. Designs of shed can have varying ratios between creepage distance to axial length [20], designs for more polluted environment have bigger ratios.

According to the typical value to calculate the creepage distance, for a 275kV design, the creepage distance required is 9625mm. Where the designs of bushing in this report has axial length of approximately 3m, the ratio of minimum nominal creepage distance to axial length required is 3.2:1. This is satisfied by many shedding designs, including the ABB GOE design with a ratio of 4.0:1 and the GOE2 design with a ratio of 3.94:1 [20].

These shed provides a greater creepage distance to reduce the chance of surface flashover, however, they have little affect on the electric field of the bushing. Hence, addition of shed does not reduce corona discharge.



(a) Air side axial electric field



(b) Oil side axial electric field

Figure 7.8: Electric field at the edge of each foil.

## 7.5 Design Improvements

The high electric field at the tips of the foils has been identified as a cause for concern. The field strength at this point exceeds the PD inception voltage by double in the axial design, and around

four times in the radial design. It is therefore necessary to improve the base design.

The first aspect to consider is the accuracy and relevance of the COMSOL model. The very thin foils are modelled as perfect rectangles with sharp  $90^\circ$  corners. This approximation was made to make the geometry of the model simple for input to COMSOL. Sharp corners cause areas of exceedingly high field strengths. A refined model was required, to confirm that the unrealistic sharp corners on the foils were not causing the exceedingly high field strengths.

The radial model was taken forward, since it already passes the radial field criteria. If a way to reduce the field at the foil tips could be found, the radial design would pass all criteria. The end of each of the foils was filleted, so that the ends formed a semi-circle. While this is still not the optimum design for an electrode, it is certainly an improvement over the sharp angles.

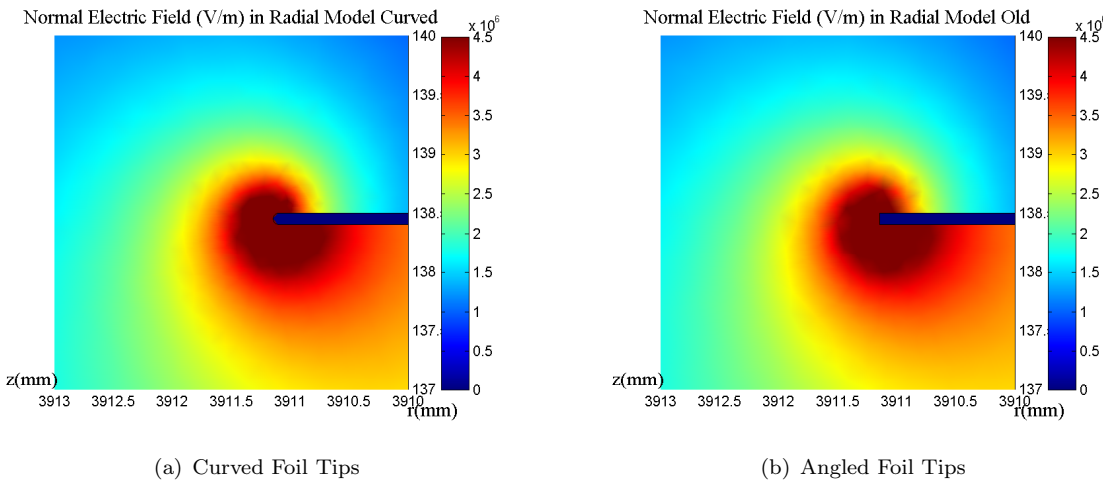


Figure 7.9: Normal Electric Field at the Tips Improvement

The curved foil tip is clearly visible in figure 7.9(a). There is an improvement, the curved design has a slightly smaller area of field strengths higher than the threshold. However, it has not solved the issue completely. Further design modifications are required.

Literature on bushing design refer to the high field at the tips problem [4]. One possible solution commonly suggested is to coat the tip of the foil in a semiconductor.

BH can you add a little bit here about the semiconductor thing - references and why would it help?

This has been modelled in COMSOL by adding a square to the edge of the foil  $0.1\text{mm}$  in dimension. The outer edges of the square are filleted to a curve in the same way the tips were previously. These squares were allocated the relative permittivity of  $\epsilon_r = 11.7$ , which is the permittivity of silicon. The actual manufacture processes are not in the scope of this report, and different semiconductors may be used in industry. However, adding this to the COMSOL will at least prove the concept.

The semiconductor block with curved edges can be seen in figure 7.10(a). It is shown alongside the original angled design for comparison in figure 7.10(b). Once again, there is a subtle improvement in the area exposed to very high field concentrations. However, it remains well above the  $4.5\text{kV/mm}$  threshold value.

The normal electric field values have been extracted and plotted in figure 7.11 to enable a more direct, quantitative comparison. It is clear that the radial semiconductor tipped model has reduced the field

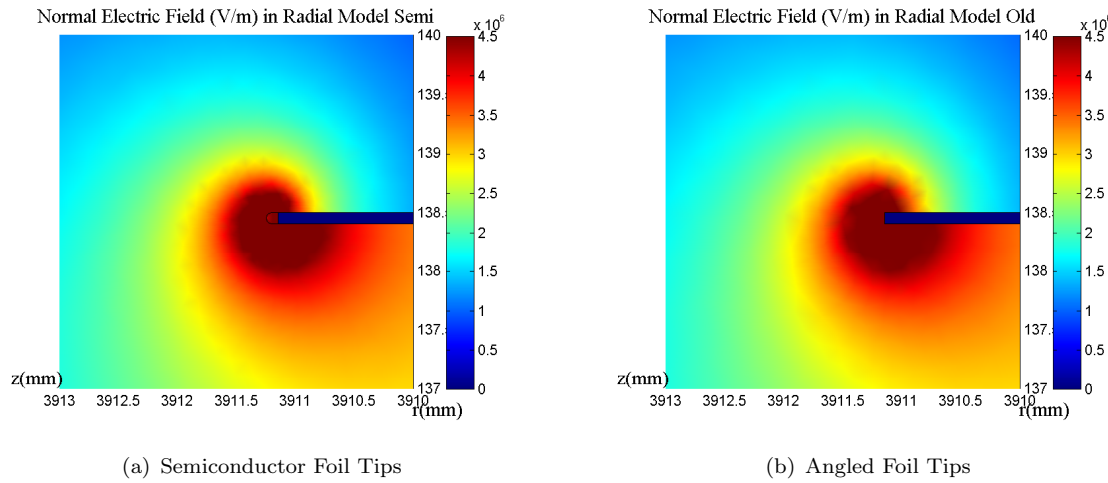


Figure 7.10: Normal Electric Field at the Tips Improvement

strength by almost half, and is nearly at the same level as the axial field design. The curved foil design is an improvement, but the semiconductor design has a significant impact on the field distribution.

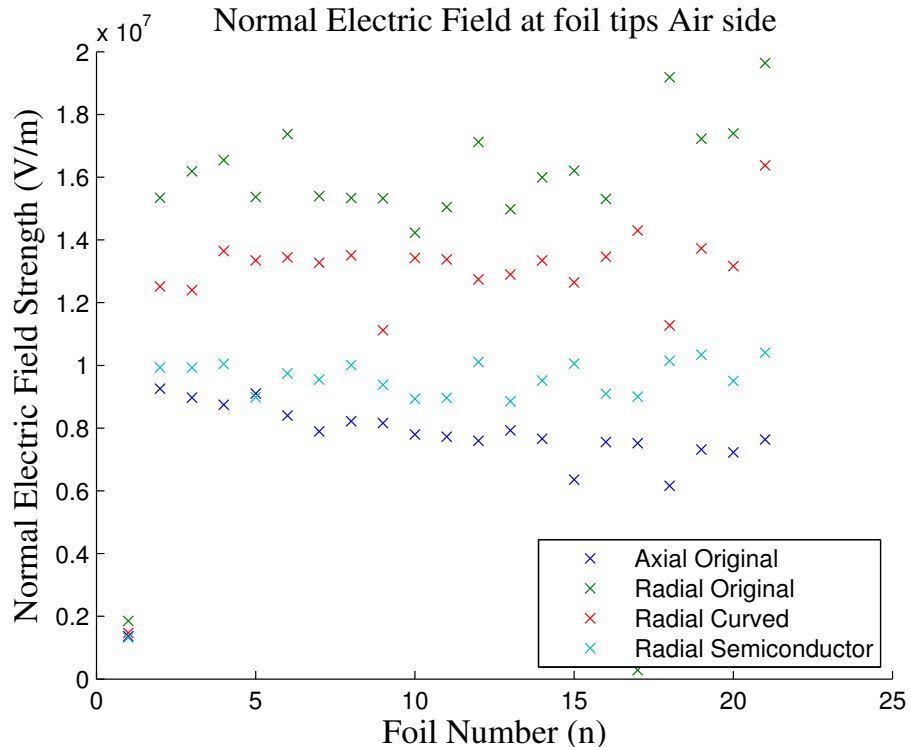


Figure 7.11: Scatter showing the normal electric field at the tips of each foil in the axial, radial, radial curved and radial semiconductor models.

## 7.6 Choice of Design

From the results shown in the previous sections, the graph of variation in radial electric field shows the peak radial electric field for the axial graded design, the limit of 4.5kV/mm is just exceeded. The radial electric in the radial grading design is consistently below the 4.5kV/mm limit.

However, the axial electric field in both design exceeds the threshold consistently. More importantly, the axial electric field for the radial graded design is in general approximately twice as much as the axial graded design, although this was improved using semiconductor tips. Hence, the results show the radial design suppresses more in radial electric field, while the axial electric field is suppressed more in the axial graded design as expected.

The choice of design depends on the effect of the axial and the radial electric field. According to the weakness for bushing designs, the axial electric field usually cause more problems as the breakdown within foil would require a higher electric field than surface discharge along the boundary layer. Using the semiconductor coated foil tips as proven in the radial design could further improve the axial field in the axial design. The choice of bushing would therefore be an axial grading design, using semiconductor coated tips.

## 8 Conclusions

All different designing methods in bushing design are about suppressing the intensity of electric field throughout the system as these intensification of electric field causes the various types of breakdown.

In relatively lower voltages high voltage systems, the use of internal and external screening electrodes might be sufficient to suppress the effect of electric field intensification. Whilst for high voltage DC systems, resistive grading method might be used to control the electric field.

Focusing on high voltage AC bushing designs, capacitive grading methods are used typically used to control the electric field distribution along the desired boundaries. This control of electric field based on the condition of constant electric field across desire points in the bushing, this condition is the basis of both the grading method and both grading methods are derived from this condition in this report. In satisfying the condition of constant electric field across the desire points in the bushing design, changes are made to the foils separation distance or the change in radius between the consecutive foils. The resultant electric field distribution in the graded direction in the simulations is not strictly linear, but close to a linear line.

By controlling the electric field, evenly distributed electric field can be achieved. Also, depending on the type of grading method used, suppression of peak in the specific component of electric field is achieved. Beside the grading methods, some other additions to the bushing design have been put forward to reduce the intensification of the electric field at the edges of the foils. Foils made from semiconducting materials can be used to adapt the potentials at the foil edges to a less concentrated field distribution [4], though installation is not mentioned. The second improvement is to fold the corners of the foil to reduce electrical tensions and optimise electric field intensity [21]. By removing the sharp edges of the foils, responsible for the localised electrical fields, the electric field distribution will be more uniform and better fit the base theory.

this  
sounds  
a bit  
weird

## References

- [1] D.F. Warne. *Newnes Electrical Power Engineer's Handbook*. Elsevier Science, 2005.
- [2] R.E. James, Q. Su, and Institution of Engineering and Technology. *Condition Assessment of High Voltage Insulation in Power System Equipment*. IET power and energy series. Institution of Engineering and Technology, 2008.

- [3] Ieee standard general requirements and test procedure for power apparatus bushings. *IEEE Std C57.19.00-2004 (Revision of IEEE Std C57.19.00-1991)*, pages 1–17, 2005.
- [4] J. Kuffel, E. Kuffel, and W.S. Zaengl. *High Voltage Engineering Fundamentals*. Elsevier Science, 2000.
- [5] Captured lightning - lichtenberg figures. [Online] Available: <http://damnamazing.blogspot.co.uk/2008/11/captured-lightning-lichtenberg-figures.html>, last viewed on 25.3.2014, 2008.
- [6] J.S. Graham. *High-Voltage Engineering and Testing, 3rd Edition*. IET Power and Energy Series, 2013.
- [7] J.H. Harlow. *Electric Power Transformer Engineering*. The Electric Power Engineering Hbk, Second Edition. Taylor & Francis, 2004.
- [8] International Electrotechnical Commission. *Insulated Bushings for Alternating Voltages Above 1000 V (IEC 60137, Ed. 5.0 (2003) MOD)*. 2008.
- [9] High-voltage test techniques partial discharge measurements. *BS EN 60270:2001*, 2001.
- [10] Hulya Kirkici. Surface flashover characteristics of dielectric thin films in vacuum: A review. *ELECO'99 International Conference on Electrical and Electronics Engineering*, page 46, 1999.
- [11] Ghosh P.S. Ghani A. Thayoob, Y.H.M. Frequency spectral analysis of electrical partial discharge signals in xlpe cable under various soil conditions. *In Power and Energy Conference*, pages 1528–1531, 2008.
- [12] Goldman A. Sigmund R.S. Goldman, M. The corona discharge, its properties and specific uses. *Pure & Appl. Chem.*, Vol. 57, No. 9, pages 1353–1362, 1985.
- [13] Zeeshan Ahmed. Analysis of partial discharge in OIP bushing models. Master's thesis, Royal Institute of Technology (KTH), September 2011.
- [14] H Rodrigo, L Graber, DS Kwag, DG Crook, and B Trociewitz. Comparative study of high voltage bushing designs suitable for apparatus containing cryogenic helium gas. *Cryogenics*, 57:12–17, 2013.
- [15] Fachgebiet Hochspannungstechnik Technische Universitt Darmstadt. Measures for field and potential control. [Online] Available: [http://www.hst.tu-darmstadt.de/uploads/media/hvt2\\_v\\_02.pdf](http://www.hst.tu-darmstadt.de/uploads/media/hvt2_v_02.pdf), last viewed on 23.12.2014.
- [16] George Chen. ELEC6089 High Voltage Insulation Systems Assignment 1 HV AC 275kV Bushing Design Briefing Notes, February 2014. The University of Southampton.
- [17] COMSOL. *Introduction to AC/DC Module - COMSOL Version 4.3*. Part No. CM020104, 2012.
- [18] Mohammad R Meshkatoddini. Study of the electric field intensity in bushing integrated zno surge arresters by means of finite element analysis. In *COSMOL Users Conference*, 2006.
- [19] W.H. Hayt and J.A. Buck. *Engineering Electromagnetics*. MCGRaw-HILL Higher Education, 2012.
- [20] Transformer bushings, type goe and goe(2), technical guide. [Online] Available: [http://www05.abb.com/global/scot/scot252.nsf/veritydisplay/60f3cd5c2edf5ff4c125771b002dbef1/\\$file/1ZSE%202750-105%20en%20Rev%207%20\(GOE\).pdf](http://www05.abb.com/global/scot/scot252.nsf/veritydisplay/60f3cd5c2edf5ff4c125771b002dbef1/$file/1ZSE%202750-105%20en%20Rev%207%20(GOE).pdf), last viewed on 23.03.2014, 2010.

- [21] Hafezinasab H. Karimi Madahi S.S. Majid Alambeygi Hassani, M. Optimization of electric field in 230kv power transformers bushing. *J. Basic. Appl. Sci. Res.*, Vol. 2, No. 5, pages 4939–4951, 2012.

## A Individual Contributions

| Team Member                    | Contribution   |
|--------------------------------|--|
| Thomas J. Smith<br>23914254    | COMSOL modelling of all designs. Sole author of section 1, 6 and 7.5. Co-author of section 3 and 4. Project manager. |
| David Mahmoodi<br>99999999     | Derivation of equations from the texts. Matlab script author. Sole author of section 5 and co-author of 3 and 4.     |
| Brendan Hickman<br>99999999    | Co-author of section 2 and 7.  |
| Patrick P. L. Fong<br>23875771 | Co-author of section 2, 3 and 7. Author of 8?  |

Conclusion and Abstract - who did those

## B Code Listings

### Radial Grading Matlab Code

```

1 %%%%%%%%%%%%%%%%%%%%%%%%%%%%%%%%%%%%%%
2 % ELEC6089 High Volatage Insulation Bushing Design
3 % Radial grading calculation
4 % Author - David Mahmoodi
5 % Date - 14/02/2014
6 %%%%%%%%%%%%%%%%%%%%%%%%%%%%%%%%%%%%%%
7 clc; close all; clear all
8 %% Declaring Given Variables
9 Voltage = 275000;
10 Inner_diameter = 100;
11 Outer_diameter = 300;
12 First_foil_length = 5000;
13 N = 21;
14 Foil_Thickness = 0.1;
15 First_Gap = 2;
16 Last_Gap = 2;
17 %% Defining new variables
18 Del_Voltage = Voltage/N-1; %Voltage between each foil
19 Del_Radius = ((Outer_diameter- Inner_diameter)-2*(First_Gap+Last_Gap))/(2*(N-1)); % Spacing between each foil
20 %Initialise vectors (22 for 3D plotting)
21 L = zeros(1,N+1);
22 Radius = zeros(1,N+1);
23 %% Calculation
24 L(1)=First_foil_length; %The first foil is 5000mm and connected to the conductor, no capacitance between
25 % conductor and this foil
26 r0 = Inner_diameter/2; %Radius of the conductor
27 Radius(1)= Inner_diameter/2 + First_Gap; % Radial position of first foil = 52mm
28 %Calculate the radial positions of all foils
29 for i=2:N
30     Radius(i)=Radius(i-1) + Del_Radius;
31 end
32 % Refer to Section 2.2 for an explanation of this assumption
33 L(2)= log(Radius(2)/Radius(1))* L(1) / log(Radius(1)/(Radius(1)-Del_Radius)) ;
34 %Follow the iterative formula
35 for i=3:N
36     L(i)= log(Radius(i-1)/Radius(i))* L(i-1) / log(Radius(i-2)/Radius(i-1));
37 end
38 %For plotting - add the outer shell
39 L(N+1)=L(N) - .5*L(N);
40 Radius(N+1)=Radius(N)+ Last_Gap;
41 %% Plotting
42 figure
43 plot(Radius(1:end-1),((6000+L(1:end-1))/2), 'o'); hold on
44 plot(Radius(1:end-1),((6000-L(1:end-1))/2), 'o');%axis equal
45 x=zeros(1,2*(N+1));
46 y=x; j=1;
47 for i=1:2:2*(N+1)
48     x(i)=L(j)/2;
49     x(i+1)=-L(j)/2;
50     y(i)=Radius(j);
51     y(i+1)=Radius(j);
52     j=j+1;
53 end
54 y2=-y;
55 % 2D Plot
56 figure
57 axes('FontSize',16,'fontWeight','bold')
58 rect_H = rectangle('Position', [-1.1.*x(1),- r0, 2.2*x(1), 2*r0]);
59 set(rect_H, 'FaceColor', 'r')
60 for i=1:2:2*(N)
61     hold on
62     line(x(i:i+1), y(i:i+1), 'LineWidth',2)
63     line(x(i:i+1), y2(i:i+1), 'LineWidth',2)
64     %axis equal
65 end
66 rect_H = rectangle('Position', [-L(N+1)/2,Outer_diameter/2, L(N+1), 10]);
67 set(rect_H, 'FaceColor', [0, 0, 0])
68 rect_H = rectangle('Position', [-L(N+1)/2,-10-Outer_diameter/2, L(N+1), 10]);
69 set(rect_H, 'FaceColor', [0, 0, 0]);
70 title('Radial Grading', 'FontName', 'Times New Roman', 'FontSize',34,'fontWeight','bold');
71 xlabel('Length (mm)', 'FontName', 'Times New Roman', 'FontSize',24,'fontWeight','bold')
72 ylabel('Radius (mm)', 'FontName', 'Times New Roman', 'FontSize',24,'fontWeight','bold')
73 xlim([x(2) x(1)]); ylim([y2(end)-10 y(end)+10])
74 %% 3D Plot
75 K=50; scl=.1; % Z direction scaling value for plotting
76 p= 6*N/3+1; %adjusting the Cut in the 3D shape
77 figure
78 axes('FontSize',16,'fontWeight','bold');
79 R=[r0 r0];
80 [X,Y,Z] = cylinder(R,5*K);
81 Z(2, :) =( L(1)+ .1*L(1))*scl;
82 Z(1, :) = - Z(2, :);
83 surf(X,Y,Z, 'FaceColor',[1,0,0], 'EdgeColor', [1,0,0]);
84 for i=1:N
85     hold on
86     R=[Radius(i) Radius(i)];
87     [X,Y,Z] = cylinder(R,K);
88     Z(2,:)= L(i);
89 end

```

```

90 Z(1,:)= -L(i);
91 X = X(:,1:p);
92 Y = Y(:,1:p);
93 Z = Z(:,1:p)*scl;
94 testsubject = surf(X,Y,Z);
95 set(testsubject, 'FaceAlpha',0.6, 'EdgeColor', 'b')
96 axis equal
97 end
98 Ground=Radius(N+1)-1;
99 for i=1:30
100 R=[Ground+i Ground+i];
101 [X,Y,Z] = cylinder(R,K);
102 Z(2, :) = L(N+1)*scl;
103 Z(1, :) = - Z(2, :);
104 X = X(:,1:p);
105 Y = Y(:,1:p);
106 Z = Z(:,1:p)*scl;
107 surf(X,Y,Z, 'FaceColor', [0,0,0], 'EdgeColor',[0, 0, 0]);
108 end
109 camlight
110 lighting gouraud
111 title('Radial Graing ', 'FontName', 'Times New Roman', 'FontSize', 24, 'fontWeight', 'bold');
112 xlabel('R(mm)', 'FontName', 'Times New Roman', 'FontSize', 16, 'fontWeight', 'bold', 'Rotation', 90, 'HorizontalAlignment', 'right')
113 zlabel('L(cm)', 'FontName', 'Times New Roman', 'FontSize', 16, 'fontWeight', 'bold', 'HorizontalAlignment', 'right')
114 %% Saving results to file
115 FID = fopen('RadialVals21.tex', 'w');
116 fprintf(FID, '\\begin{table}![htb]\\n');
117 fprintf(FID, '\\begin{center}\\n');
118 fprintf(FID, '\\begin{tabular}{|c||cc|c||cc|}\\n');
119 fprintf(FID, '\\toprule\\n');
120 fprintf(FID, '\\textbf{Foil N.O} & \\textbf{Radius(mm)} & \\textbf{Length(mm)} & \\textbf{Foil N.O} & \\textbf{Radius(mm)} & \\textbf{Length(mm)}\\\\\\toprule\\n');
121 Max = floor((N+1)/2); L(N+1)= 00;
122 for i=1:Max
123 fprintf(FID, '%.f & %.4f & %.4f & %.4f & %.4f & %.4f \\n', i, Radius(i), L(i), (i+Max), Radius(i+Max), L(i+Max));
124 end
125 fprintf(FID, '\\bottomrule\\n');
126 fprintf(FID, '\\end{tabular}\\n');
127 fprintf(FID, '\\end{center}\\n');
128 fprintf(FID, '\\caption{Radial Grading Calculations Results}\\n');
129 fprintf(FID, '\\label{table:radialvals}\\n');
130 fprintf(FID, '\\end{table}\\n');
131 fclose(FID);
132
133 SID = fopen('Radial-Points-Air.txt', 'w');
134 for i=1:N
135 fprintf(FID, '%f\t%f\t\r\\n', Radius(i), 3000.01+(L(i)/2));
136 end
137 fclose(SID);
138 SID = fopen('Radial-Points-Oil.txt', 'w');
139 for i=1:N
140 fprintf(FID, '%f\t%f\t\r\\n', Radius(i), 2999.99-(L(i)/2));
141 end
142 fclose(SID);

```

## Axial Grading Matlab Code

```

1 %%%%%%%%%%%%%%%%%%%%%%%%%%%%%%%%%%%%%%%
2 % ELEC6089 High Volatage Insulation Bushing Design
3 % Axial grading calculation
4 % Author - David Mahmoodi
5 % Date - 14/02/2014
6 %%%%%%%%%%%%%%%%%%%%%%%%%%%%%%%%%%%%%%%
7 clc; close all; clear all
8 %% Declareing Given Variables
9 Voltage = 275000; %Applied voltage (volt)
10 Inner_diameter = 100; %mm
11 Outer_diameter = 300; %mm
12 First_foil_length = 5000; %mm
13 N = 21;
14 Foil_Thickness = 0.1; %mm
15 First_Gap = 2; %mm
16 Last_Gap = 2; %mm
17 E_boundary_surface_Air = 300; %volt/mm
18 E_boundary_surface_Oil = 3*300; %volt/mm
19 %% Defining new variables
20 Del_Voltage = Voltage/N-1; %Voltage between each foil
21 b_Air = Del_Voltage/E_boundary_surface_Air;
22 b_Oil = Del_Voltage/E_boundary_surface_Oil;
23 %Initialise vectors (22 for 3D plotting)
24 L = zeros(1,N+1);
25 L_Air = zeros(1,N+1);
26 L_Oil = zeros(1,N+1);
27 Radius = zeros(1,N+1);
28 R_parameter=1.007; % Parameter for adjecting assumption value of r0
29 %% Calculation
30 L(1)=First_foil_length; %The first foil is 5000mm and connected to the conductor, no capacitance between
  conductor and this foil
31 r0 = Inner_diameter/2 ; %Radius of the conductor
32 Radius(1)= Inner_diameter/2 + First_Gap; % Radial position of first foil = 52mm
33 L_Air(1)= L(1)/2;
34 L_Oil(1)= L(1)/2;

```

```

35 %Calculate the radial positions of all foils
36 for i=2:N
37     L_Air(i)=L_Air(i-1)- b_Air;
38     L_Oil(i)=L_Oil(i-1)- b_Oil;
39     L(i)= L_Air(i)+L_Oil(i);
40 end
41 % Refer to Section 2.2 for an explanation of this assumption
42 Radius(2)= Radius(1)* exp( (L(2)/L(1)) * log(Radius(1)/(r0-R_parameter)));
43 %Follow the iterative formula
44 for i=3:N
45     Radius(i)= Radius(i-1)* exp( (L(i)/L(i-1)) * log(Radius(i-1)/Radius(i-2)));
46 end
47 %For plotting - add the outer shell
48 L(N+1)=L(N)- .5*L(N);
49 Radius(N+1)=Radius(N)+ Last_Gap;
50
51 %% Ploting
52 figure
53 plot(Radius(1:end-1),3000+L_Air(1:end-1), 'o'); hold on %axis equal
54 plot(Radius(1:end-1),3000-L_Oil(1:end-1), 'o'); %axis equal
55 x=zeros(1,2*(N+1));
56 y=x; j=1;
57 for i=1:2:2*(N+1)
58     x(i)=L_Air(j);
59     x(i+1)=-L_Oil(j);
60     y(i)=Radius(j);
61     y(i+1)=Radius(j);
62     j=j+1;
63 end
64 y2=-y;
65 % 2D Plot
66 figure
67 axes('FontSize',16, 'fontWeight', 'bold')
68 rect_H = rectangle('Position', [-1.1*x(1), -r0, 2.2*x(1), 2*r0]);
69 set(rect_H, 'FaceColor', 'r')
70 for i=1:2:2*(N)
71     hold on
72     line(-x(i:i+1), -y(i:i+1), 'LineWidth', 2)
73     line(-x(i:i+1), -y2(i:i+1), 'LineWidth', 2)
74     %axis equal
75 end
76 rect_H = rectangle('Position', [L(N+1)/3, Outer_diameter/2, L(N+1)/2, 1000]);
77 set(rect_H, 'FaceColor', [0, 0, 0])
78 rect_H = rectangle('Position', [L(N+1)/3, -10-Outer_diameter/2, L(N+1)/2, 10]);
79 set(rect_H, 'FaceColor', [0, 0, 0])
80 title('Axial Graing', 'FontName', 'Times New Roman', 'FontSize', 34, 'fontWeight', 'bold');
81 xlabel('Length (mm)', 'FontName', 'Times New Roman', 'FontSize', 24, 'fontWeight', 'bold');
82 ylabel('Radius (mm)', 'FontName', 'Times New Roman', 'FontSize', 24, 'fontWeight', 'bold');
83 xlim([x(2) x(1)]); ylim([y2(end)-10 y(end)+10])
84 % 3D Plot
85 K=50; scl=1.1; % Z direction scaling value for plotting
86 p= 6*N/3+1; %adjusting the Cut in the 3D shap
87 figure
88 axes('FontSize',16, 'fontWeight', 'bold')
89 R=[r0 r0];
90 [X,Y,Z] = cylinder(R,5*K);
91 Z(2, :) = (L_Air(1)+ .1*L_Air(1))*scl;
92 Z(1, :) = - Z(2, :);
93 surf(X,Y,Z, 'FaceColor', [1,0,0], 'EdgeColor', [1,0,0]);
94 for i=1:N
95     hold on
96     R=[Radius(i) Radius(i)];
97     [X,Y,Z] = cylinder(R,K);
98     Z(2,:)= L_Air(i);
99     Z(1,:)= -L_Oil(i);
100    X = X(:,1:p);
101    Y = Y(:,1:p);
102    Z = Z(:,1:p)*scl;
103    testsubject = surf(X,Y,Z);
104    set(testsubject, 'FaceAlpha', 0.8, 'EdgeColor', 'b')
105    axis equal
106 end
107 Ground=Radius(N+1)-1;
108 for i=1:30
109     R=[Ground+i Ground+i];
110     [X,Y,Z] = cylinder(R,K);
111     Z(2, :) = L(N+1) *scl;
112     Z(1, :) = - Z(2, :);
113     X = X(:,1:p);
114     Y = Y(:,1:p);
115     Z = Z(:,1:p)*scl-100;
116     surf(X,Y,Z, 'FaceColor', [0,0,0], 'EdgeColor', [0, 0, 0]);
117 end
118 camlight
119 lighting gouraud
120 title('Axial Graing', 'FontName', 'Times New Roman', 'FontSize', 24, 'fontWeight', 'bold');
121 xlabel('R(mm)', 'FontName', 'Times New Roman', 'FontSize', 16, 'fontWeight', 'bold', 'Rotation', 90, 'HorizontalAlignment', 'right')
122 zlabel('L(cm)', 'FontName', 'Times New Roman', 'FontSize', 16, 'fontWeight', 'bold', 'HorizontalAlignment', 'right')
123 %% Saving results to file
124 FID = fopen('AxialVals21.tex', 'w');
125 fprintf(FID, '\\begin{table}![htb]\\n');
126 fprintf(FID, '\\begin{center}\\n');
127 fprintf(FID, '\\begin{tabular}{|c||cc|c||cc|}\\n');
128 fprintf(FID, '\\toprule\\n');
129 fprintf(FID, '\\textbf{Foil N.O.} & \\textbf{Radius(mm)} & \\textbf{Length(mm)} & \\textbf{Foil N.O.} & \\textbf{Radius(mm)} & \\textbf{Length(mm)}\\\\\\toprule\\n');

```

```
130 Max = floor((N+1)/2); L(N+1)= 00;
131 for i=1:Max
132     fprintf(FID, '%.f & %4.2f & %4.2f & %.f & %4.2f & %4.2f & %4.2f \\\n', i,Radius(i),L(i),(i+Max),Radius(i+Max),L
133     (i+Max));
134 end
135 fprintf(FID, '\\bottomrule\n');
136 fprintf(FID, '\\end{tabular}\n');
137 fprintf(FID, '\\caption{Axial Grading Calculations Results}\n');
138 fprintf(FID, '\\label{table:axialvals}\n');
139 fprintf(FID, '\\end{table}\n');
140 fclose(FID);
141
142 SID = fopen('Axial-Points-Air.txt', 'w');
143 for i=1:N
144     fprintf(FID, '%f\t%f\t\r\n', Radius(i),3000.1+L_Air(i));
145 end
146 fclose(SID);
147 SID = fopen('Axial-Points-Oil.txt', 'w');
148 for i=1:N
149     fprintf(FID, '%f\t%f\t\r\n', Radius(i),2999.9-L_Oil(i));
150 end
151 fclose(SID);
```

---